Process systems modelling and applications in granulation: A review

I.T. Cameron[a],[*], F.Y. Wang[a], C.D. Immanuel[b], F. Stepanek[b]

[a]*Particle & Systems Design Centre, School of Engineering, The University of Queensland, Brisbane, Qld. 4072, Australia*
[b]*Department of Chemical Engineering and Chemical Technology, Imperial College of Science, Technology and Medicine, London, UK*

Abstract

Granulation is one of the fundamental operations in particulate processing and has a very ancient history and widespread use. Much fundamental particle science has occurred in the last two decades to help understand the underlying phenomena. Yet, until recently the development of granulation systems was mostly based on popular practice. The use of process systems approaches to the integrated understanding of these operations is providing improved insight into the complex nature of the processes.

Improved mathematical representations, new solution techniques and the application of the models to industrial processes are yielding better designs, improved optimisation and tighter control of these systems. The parallel development of advanced instrumentation and the use of inferential approaches provide real-time access to system parameters necessary for improvements in operation. The use of advanced models to help develop real-time plant diagnostic systems provides further evidence of the utility of process system approaches to granulation processes. This paper highlights some of those aspects of granulation.
© 2005 Elsevier Ltd. All rights reserved.

Keywords: Granulation; Systems engineering; Modelling; Dynamic simulation; Control; Population balance

0. Introduction

Process systems engineering (PSE) provides a unifying paradigm for the representation, analysis and development of industrially relevant operations. It is this perspective which is discussed in this review paper on granulation processes. The importance of the process systems perspective is that the basic science of particulate systems can be usefully integrated into the "bigger picture".

A systems approach allows both the researcher and the practitioner to address key challenges at different levels of detail—a so-called multiscale approach, as well as considering the process lifecycle—from concept and research through design, operation and decommissioning. Underlying nearly all modern systems approaches are the appropriate representations to be used—a "model-centric" approach. These are the system models which figure prominently in the following sections, where they form the basis for dynamic analysis, control, optimisation and diagnosis.

Michaels (2003) has pointed out that despite the change of particle technology from an under-funded and widely scattered research enterprise to a thriving globally recognised engineering discipline over the past 25 years, design and analysis of industrial particulate processes remain rooted in empiricism. Without exception, granulation processes, like most solid-handling operations, continues to be one of the least understood and hence inefficient processes in the process industries. Thus, granulation remained more of "an art than a science" until a decade ago, as stated by Litster (2003). Granulation operations were performed employing popular practice rather than through systematic scientifically-based strategies. The ineffectiveness of this approach led researchers into a quest to systematise the design and operation of granulation processes, leading to a more systems engineering approach to this problem.

As indicated in the outline above, systems approaches to granulation operation normally entail the mathematical modelling of the process and the use of models in both

---

[*] Corresponding author. Tel.: +61 7 3365 4261; fax: +61 7 3365 4199.
E-mail address: itc@uq.edu.ac (I.T. Cameron).

off-line optimisation and on-line monitoring and control. Thus, the models serve as both a diagnosis tool and as a tool for day-to-day effective operation and control. In addition, the model can be used to aid in the study of the process mechanisms; in the evaluation of the sensitivities and controllability of the processes; and in systematising the product and process design. Further, the granulation process presents excellent challenges in multiscale modelling, optimisation and control, depending upon the objectives that are of interest to the practitioner. Each of these factors is elaborated upon in this document.

1. Multiscale, process systems aspects of granulation

Multiscale systems and hence their models exist due to the phenomena that they contain or seek to represent. This is due to the fact that thermodynamic behaviour and rate processes constitute our main view of the scientific and engineering world.

Within process engineering, the multiscale approach facilitates the discovery and manufacture of complex products. These may have *multiscale product specifications*, that is, desired properties specified at different scales. Biotechnology, nanotechnology and particulate technology—in fact, product engineering in general—are driving the interest in the multiscale approach (Villermaux, 1996; Charpentier, 2002; Cussler and Wei, 2003). The traditional approaches to studying particle technology are typically focused on two length scales: the macro-scale (unit operation level), and the micro-scale (particle level), with little efforts spent on the intermediate scale (Michaels, 2003). Advances in the design, optimisation and control of particulate processes require filling of this gap in knowledge.

The development of granulation processes via drum or pan granulation is a multiscale operation, where final product quality is determined not only by the macro scale processing equipment level but also at the micro scale level of particle formation and interaction. A typical granulation circuit diagram consists of the granulator where fine feed or recycle granules are contacted with a binder or reaction slurry. Growth occurs depending on a number of operational and property factors. Drying, product separation and treatment of recycle material then occur. For this application Fig. 1 shows a scale map from Ingram and Cameron (2002) which considers the key phenomena as represented by length and time scales within the processes. The scales represent individual particles through to agglomerates and then onto processing equipment and finally the complete circuit.

Fig. 2 shows the key processes in granulation with a schematic illustration of information links between adjacent scales. Interaction between scales is typically bidirectional.

2. Modelling of granulation systems

Modelling underlies nearly all systems approaches to the representation and exploitation of process characteristics.
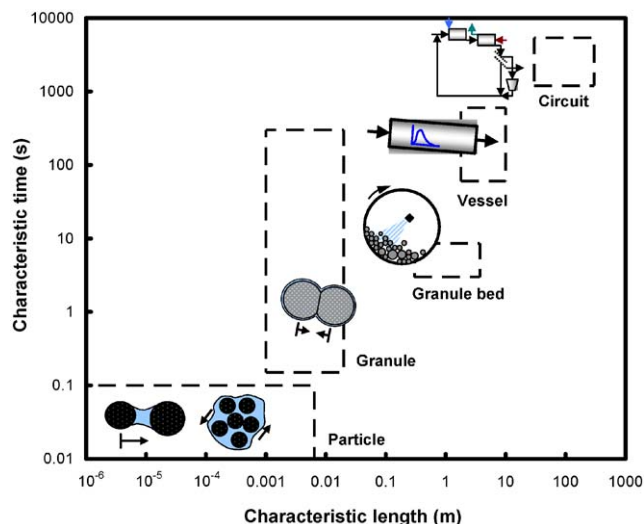

Fig. 1. Multiscale map of granulation systems (Ingram and Cameron, 2002).
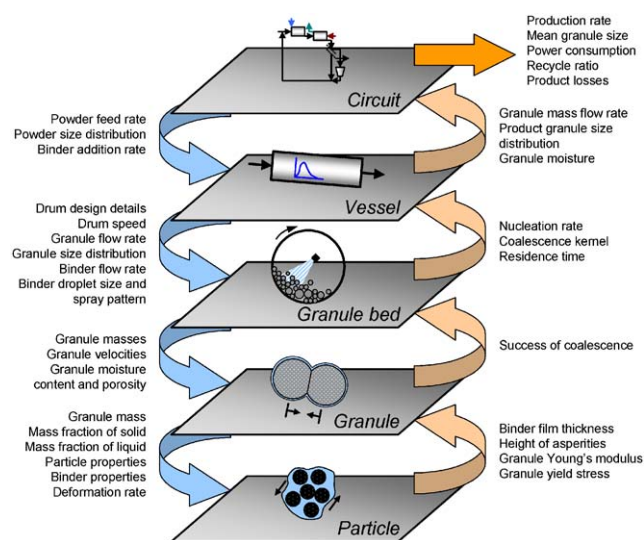

Fig. 2. Multiscale processes in granulation (Ingram and Cameron, 2002).

Granulation processes are no exception and the following sections review past and current work that has taken place in modelling these processes (Cameron and Wang, 2005).

2.1. Approaches to modelling

There are several approaches to modelling process systems. At one extreme we have mechanistic modelling that seeks to incorporate the fundamental physics and chemistry into the model. This is the so-called "white box" approach. At the other end of the spectrum we have the fitting of an arbitrary function to the input-output data—the empirical model. In between we have the so-called "grey box" models, which are normally what is developed. These three approaches to process modelling are discussed in detail

by Hangos and Cameron (2001). Some relevant comments follow.

2.1.1. Empirical or black box methods

These models are based on actual plant data, typically in the form of time series of input and output data at fixed time intervals. The model is built by selecting a model structure M and then fitting the model parameters to get the best fit of the model to the data. Model forms such as auto-regressive moving average (ARMA) or ARMAX (X = exogenous) types are typically used.

In most cases, techniques are used to vary both the structure and the model parameters to obtain the "best" or simplest model that gives the "best" fit. Various information criteria like Akaike's (1970) or Bayesian measures (Breipohl, 1970) can be used that essentially get the simplest model for the best fit. It is a form of parsimony in model building.

This approach can be very useful if no significant insight is needed into the model but a model is needed quickly to be used for a control application. The structural form of the model and the parameter values normally have no physical significance. The application range of such a model is limited to the range of data and hence this can be a significant limitation.

2.1.2. Mechanistic and grey-box models

Mechanistic models incorporate the underlying understanding of the physics and chemistry into the models. Typically we can identify two major aspects in mechanistic modelling that cover conservation and constitutive aspects:

- Application of thermodynamic conservation principles for mass, energy and momentum and,
- Application of population balances that track particle size distributions as various particulate phenomena take place.
- Development of appropriate constitutive relations that define intensive properties, mass and heat transfer mechanisms as well as particle growth and breakage mechanisms.

The development of mechanistic models is far more complex and time-consuming than for empirical models and is only justified when time permits, the model is to be used over a wide operating range and the relevant insight in establishing the constitutive relations is available.

Inevitably, even the best mechanistic models require some data fitting, leading to the concept of "grey box" models. This is the normal practice in modelling of such systems. It means that adequate data must be available to carry out the validation studies. This task is particularly difficult for validation of dynamic models.

2.2. The principal mechanisms in granulation modelling

There are three principal mechanisms that need to be considered, which have been reviewed by Iveson et al. (2001).

2.2.1. Nucleation

Nucleation refers to the formation of initial aggregates that are typically a result of interaction between the binder spray droplets and the powder in the device. This mechanism provides the initial stage for further growth through a number of mechanisms. A number of nucleation models have been proposed in the literature. (Wildeboer, 2002).

2.2.2. Growth

Granule growth occurs through two key mechanisms that can be separated for discussion purposes. The topic is discussed more fully in Sections 2.3.2 and 5.3.2.

2.2.2.1. Layering

Layering refers to the take up of fine particles onto the surface of larger granules. It is often induced by rolling action and is a means of granule growth that creates hard, compact granules. A practical layering model is proposed in Section 5.3.2 for solving optimal control of granulation processes.

2.2.2.2. Agglomeration

Agglomeration or coalescence refers to the successful collision of two particles that result in a composite particle. The success of collisions can be a function of particle size, binder and powder properties and operational factors such as bed height, powder velocity and shear for mixer granulators. See Sections 2.3.2 and 5.3.2 for more details.

2.2.3. Breakage

Breakage in high shear and drum granulation is a significant issue, being more important in high shear devices. There are various forms of breakage from cleavage of particles to particle surface attrition where the granule is chipped by collision with other particles, the wall or impeller. Complexity of breakage models extends from binary breakage models to full particle distributions represented by breakage and selection functions or empirical models (Yekeler and Ozkan, 2002; Salman et al., 2002; van den Dries et al., 2003).

The following sections now discuss some of the important aspects of granulation process modelling, through the use of population balances and alternative approaches.

2.3. Representing granulation processes through population balances

The particulate nature of solids is characterised by a number of properties, such as size, shape, liquid and gas content, porosity, composition and age. These properties are denoted as internal coordinates, whereas the Euclidian coordinates, such as rectangular coordinates (x, y, z), cylindrical coordinates (r, φ, z), and spherical coordinates (r, θ, φ) used to specify the locations of particles are defined as external coordinates.

The most important property for the characterisation of particles is particle size. Randolph and Larson (1988)

pointed out that: "As no two particles will be exactly the same size, the material must be characterised by the distribution of sizes or particle-size distribution (PSD)." If only size is of interest, a single-variable distribution function is sufficient to characterise the particulate system. If additional properties are also important, multivariable distribution functions must be developed. These distribution functions can be predicted through numerical simulations using population balance equations (PBE) (Hounslow, 1998).

Ramkrishna (2000) provided a brief explanation on the population balance equation as: "The population balance equation is an equation in the number density and may be regarded as representing a number balance on particles of a particular state. The equation is often coupled with conservation equation for entities in the particles' environmental (or continuous) phase."

Both single-variable and multivariable population balances can be developed. However, the emphasis will be placed on the single-variable population balance equations with size as the only internal coordinate.

2.3.1. General population balance equations

A population balance for particles in some fixed subregion of particle phase space can be conceptually represented in natural words as follows:

$$
\begin{aligned}
&\left\{\begin{array}{l}\text{density function change}\\ \text{inclass, location \& time}\end{array}\right\}\\
&=\left\{\begin{array}{l}\text{disperse in}\\ \text{through boundary}\end{array}\right\}-\left\{\begin{array}{l}\text{disperse out}\\ \text{through boundary}\end{array}\right\}\\
&+\left\{\begin{array}{l}\text{flow in}\\ \text{through boundary}\end{array}\right\}-\left\{\begin{array}{l}\text{flow out}\\ \text{through boundary}\end{array}\right\}\\
&+\left\{\begin{array}{l}\text{grow in}\\ \text{from lower classes}\end{array}\right\}-\left\{\begin{array}{l}\text{grow out}\\ \text{from current class}\end{array}\right\}\\
&+\left\{\begin{array}{l}\text{birth due to}\\ \text{coalescence}\end{array}\right\}-\left\{\begin{array}{l}\text{death due to}\\ \text{coalescence}\end{array}\right\}\\
&+\left\{\begin{array}{l}\text{break}-\text{up in}\\ \text{from upper classes}\end{array}\right\}\\
&-\left\{\begin{array}{l}\text{break}-\text{up out}\\ \text{from current class}\end{array}\right\}
\end{aligned}\tag{2.1}
$$

The super-structure of the general population balance equation can be represented as follows:

$$
\begin{aligned}
\frac{\partial}{\partial t}f(\mathbf{x},\mathbf{r},t)=&\nabla_r\bullet\nabla_r[D_r f(\mathbf{x},\mathbf{r},t)]-\nabla_r\bullet\dot{\mathbf{R}}f(\mathbf{x},\mathbf{r},t)\\
&-\nabla_x\bullet\dot{\mathbf{X}}f(\mathbf{x},\mathbf{r},t)\\
&+B_c(\mathbf{x},\mathbf{r},t)-D_c(\mathbf{x},\mathbf{r},t)\\
&+B_b(\mathbf{x},\mathbf{r},t)-D_b(\mathbf{x},\mathbf{r},t),
\end{aligned}\tag{2.2}
$$

where f is the multi-variant number density as a function of properties and locations, $\mathbf{r}$ is the external coordinate vector (also known as spatial coordinate vector) for the determination of particle locations, $\mathbf{x}$ is the internal coordinate vector

for the identification of particle properties, such as size, moisture content and age, D_r is the dispersion coefficient, $\dot{\mathbf{R}}$ is the velocity vector in the external coordinate system, $\dot{\mathbf{X}}$ is the rate vector in the internal coordinate system, B_c and D_c are birth and death rates for coalescence, respectively, B_b and D_b are birth and death rates for breakage, respectively. The first and second terms in the right hand side of Eq. (2.2) represent dispersion and convection particle transport, respectively, whereas the third term quantifies the growth of particles with respect to various properties, such as size and moisture. The birth and death rates for coalescence are given by

$$
\begin{aligned}
B_c(\mathbf{x},\mathbf{r},t)=&\int_{\Omega_x}\mathrm{d}V_{x'}\int_{\Omega_r}\frac{1}{\delta}\beta(\tilde{\mathbf{x}},\tilde{\mathbf{r}};\mathbf{x}',\mathbf{r}')\\
&\times f(\tilde{\mathbf{x}},\tilde{\mathbf{r}},t)f(\mathbf{x}',\mathbf{r}',t)\frac{\partial(\tilde{\mathbf{x}},\tilde{\mathbf{r}})}{\partial(\mathbf{x},\mathbf{r})}\,\mathrm{d}V_{r'},
\end{aligned}
$$

$$
\begin{aligned}
D_c(\mathbf{x},\mathbf{r},t)=&f(\mathbf{x},\mathbf{r},t)\int_{\Omega_x}\mathrm{d}V_{x'}\int_{\Omega_r}\beta(\mathbf{x}',\mathbf{r}';\mathbf{x},\mathbf{r})\\
&\times f(\mathbf{x}',\mathbf{r}',t)\,\mathrm{d}V_{r'},
\end{aligned}\tag{2.3}
$$

where β is the coalescence kernel, Ω_x and Ω_r are integration boundaries for internal and external coordinates, respectively, δ represents the number of times identical pairs have been considered in the interval of integration so that $1/\delta$ corrects for the redundancy, the term $\partial(\tilde{\mathbf{x}},\tilde{\mathbf{r}})/\partial(\mathbf{x},\mathbf{r})$ accounts for the coordinate transformation such that the colliding pair with original coordinates $[\tilde{\mathbf{x}},\tilde{\mathbf{r}}]$ and $[\mathbf{x}',\mathbf{r}']$, respectively before collision should be identified by the coordinates $[\mathbf{x},\mathbf{r}]$ after coalescence. Mathematically, this requires that the density with respect to coordinates $[\tilde{\mathbf{x}}(\mathbf{x},\mathbf{r}|\mathbf{x}'\mathbf{r}'),\tilde{\mathbf{r}}(\mathbf{x},\mathbf{r}|\mathbf{x}'\mathbf{r}')]$ must be transformed into one in terms of $(\mathbf{x},\mathbf{r})$ by using the appropriate Jacobian of the transformation. Ramkrishna (2000) showed that the determinant of the Jacobian of the transformation satisfies the following equation:

$$
\frac{\partial(\tilde{\mathbf{x}},\tilde{\mathbf{r}})}{\partial(\mathbf{x},\mathbf{r})}=\begin{vmatrix}
\frac{\partial\tilde{x}_1}{\partial x_1}&\cdots&\frac{\partial\tilde{x}_1}{\partial x_n}&\frac{\partial\tilde{x}_1}{\partial r_1}&\frac{\partial\tilde{x}_1}{\partial r_2}&\frac{\partial\tilde{x}_1}{\partial r_3}\\
\vdots&\vdots&\vdots&\vdots&\vdots&\vdots\\
\frac{\partial\tilde{x}_n}{\partial x_1}&\cdots&\frac{\partial\tilde{x}_n}{\partial x_n}&\frac{\partial\tilde{x}_n}{\partial r_1}&\frac{\partial\tilde{x}_n}{\partial r_2}&\frac{\partial\tilde{x}_n}{\partial r_3}\\
\frac{\partial\tilde{r}_1}{\partial x_1}&\cdots&\frac{\partial\tilde{r}_1}{\partial x_n}&\frac{\partial\tilde{r}_1}{\partial r_1}&\frac{\partial\tilde{r}_1}{\partial r_2}&\frac{\partial\tilde{r}_1}{\partial r_3}\\
\frac{\partial\tilde{r}_2}{\partial x_1}&\cdots&\frac{\partial\tilde{r}_2}{\partial x_n}&\frac{\partial\tilde{r}_2}{\partial r_1}&\frac{\partial\tilde{r}_2}{\partial r_2}&\frac{\partial\tilde{r}_2}{\partial r_3}\\
\frac{\partial\tilde{r}_3}{\partial x_1}&\cdots&\frac{\partial\tilde{r}_3}{\partial x_n}&\frac{\partial\tilde{r}_3}{\partial r_1}&\frac{\partial\tilde{r}_3}{\partial r_2}&\frac{\partial\tilde{r}_3}{\partial r_3}
\end{vmatrix}.\tag{2.4}
$$

The birth and death rates for breakage are described as

$$
\begin{aligned}
B_b(\mathbf{x},\mathbf{r},t)=&\int_{\Omega_r}\mathrm{d}V_{r'}\int_{\Omega_x}b(\mathbf{x}',\mathbf{r}',t)P(\mathbf{x},\mathbf{r}|\mathbf{x}',\mathbf{r}',t)\\
&\times S(\mathbf{x}',\mathbf{r}',t)f(\mathbf{x}',\mathbf{r}',t)\,\mathrm{d}V_{x'}
\end{aligned}\tag{2.5}
$$

$$
D_b(\mathbf{x},\mathbf{r},t)=S(\mathbf{x},\mathbf{r},t)f(\mathbf{x},\mathbf{r},t),\tag{2.6}
$$

where $b(\mathbf{x}',\mathbf{r}',t)$ is the average number of particles formed from the breakage of a single particle of state $(\mathbf{x}',\mathbf{r}')$ at time t, $P(\mathbf{x},\mathbf{r}|\mathbf{x}',\mathbf{r}',t)$ is the probability density

function for particle from the breakage of state $(\mathbf{x}', \mathbf{r}')$ at time t that have state $(\mathbf{x}, \mathbf{r})$, $S(\mathbf{x}, \mathbf{r}, t)$ is the selection function, which represents the fraction of particles of state $(\mathbf{x}, \mathbf{r})$ breaking per unit time.

Eqs. (2.3) and (2.4) involve three different locations: $\tilde{\mathbf{r}}$ and $\mathbf{r}'$ for the colliding pair of particles and $\mathbf{r}$ for the agglomerated particle. Although this treatment is general and mathematically rigorous, it could be unnecessarily complicated for engineering applications. A common practice is to assume that these three locations are very close to each other during the particle collision and granule formation. That is

$$\tilde{\mathbf{r}} \approx \mathbf{r}' \approx \mathbf{r}. \tag{2.7}$$

This assumption requires that the phenomenon of fast particle jumps in the system is not severe, which is achievable for most industrial granulation processes. If Eq. (2.7) holds, Eqs. (2.3) and (2.4) can be simplified considerably to obtain

$$B_c(\mathbf{x}, \mathbf{r}, t) = \frac{1}{2} \int_{\Omega_x} \beta(\tilde{\mathbf{x}}, \mathbf{x}', \mathbf{r}) \\ \times f(\tilde{\mathbf{x}}, \mathbf{r}, t) f(\mathbf{x}', \mathbf{r}, t) \frac{\partial(\tilde{\mathbf{x}})}{\partial(\mathbf{x})} \, dV_{x'}$$

$$D_c(\mathbf{x}, \mathbf{r}, t) = f(\mathbf{x}, \mathbf{r}, t) \int_{\Omega_x} \beta(\mathbf{x}', \mathbf{x}, \mathbf{r}) f(\mathbf{x}', t) \, dV_{x'} \tag{2.8}$$

$$\frac{\partial(\tilde{\mathbf{x}})}{\partial(\mathbf{x})} = \begin{vmatrix} \frac{\partial \tilde{x}_1}{\partial x_1} & \cdots & \frac{\partial \tilde{x}_1}{\partial x_n} \\ \vdots & \vdots & \vdots \\ \frac{\partial \tilde{x}_n}{\partial x_1} & \cdots & \frac{\partial \tilde{x}_n}{\partial x_n} \end{vmatrix}. \tag{2.9}$$

Similarly, Eq. (2.5) becomes

$$B_b(\mathbf{x}, \mathbf{r}, t) = \int_{\Omega_x} b(\mathbf{x}', \mathbf{r}, t) P(\mathbf{x}|\mathbf{x}', \mathbf{r}, t) \\ \times S(\mathbf{x}', \mathbf{r}, t) f(\mathbf{x}', \mathbf{r}, t) \, dV_{x'}. \tag{2.10}$$

In the following material, breakage effects have been considered negligible and Eq. (2.7) is always assumed to be valid.

2.3.2. One-dimensional (1-D) population balance models

One-dimensional population balance models for both batch and continuous systems are described in this section as special cases of the generalised population balance model.

2.3.2.1. Batch systems
For a well-mixed batch system with only one internal coordinate v (particle size), Eq. (2.2) is reduced to

$$\frac{\partial}{\partial t} n(v, t) = -\frac{\partial}{\partial v} [Gn(v, t)] \\ + \frac{1}{2} \int_0^v \beta(v - v', v') n(v - v', t) n(v', t) \, dv' \\ - n(v, t) \int_0^\infty \beta(v, v') n(v', t) \, dv', \tag{2.11}$$

where n is the one-dimensional number density, G is known as the growth rate. For notational clarity, we use f and n to denote the multi-dimensional and one-dimensional number density functions, respectively. Both notations bear the same physical significance. Through a comparison of Eq. (2.11) with Eqs. (2.2), (2.8) and (2.9), it is easy to observe the following membership relationships:

$$v \in \mathbf{x}, \quad v' \in \mathbf{x}', \quad (v - v') \in \tilde{\mathbf{x}}, \\ G = \frac{dv}{dt} \in \dot{\mathbf{X}}, \quad \frac{\partial(\tilde{\mathbf{x}})}{\partial(\mathbf{x})} = \frac{\partial(v - v')}{\partial v} = 1. \tag{2.12}$$

Eq. (2.11) is more frequently applied to industrial granulation processes than its generalised format described by Eq. (2.2).

2.3.2.2. Continuous systems
The population balance equation for continuous systems with one internal and one external coordinate is given by

$$\frac{\partial}{\partial t} n(v, z, t) \\ = -\frac{\partial}{\partial z} [\dot{Z} n(v, z, t)] - \frac{\partial}{\partial v} [Gn(v, z, t)] \\ + \frac{1}{2} \int_0^v \beta(v - v', v') n(v - v', z, t) n(v', z, t) \, dv' \\ - n(v, z, t) \int_0^\infty \beta(v, v') n(v', z, t) \, dv', \tag{2.13}$$

where the spatial velocity is defined as

$$\dot{Z} = \frac{dz}{dt} \in \dot{\mathbf{R}}. \tag{2.14}$$

Although continuous granulation processes are commonly encountered in the fertiliser and mineral processing industries, most granulation operations in the pharmaceutical industry are performed as batch processes employing either high-shear mixers or batch fluidised-bed granulators. Consequently, most modelling studies on pharmaceutical granulation have focused on batch processes.

In addition to these models for high-shear granulation, the modelling of continuous fluidised-bed spray granulation with recycle is discussed by Heinrich et al. (2003). The model successfully predicts the occurrence of both oscillatory steady states as well as unique steady states in these processes.

2.4. Coalescence kernels

The coalescence kernel is affected by two major factors: (1) collision probability of the specified pair of particles, and (2) successful coalescence or rebounding after collision. The first factor mainly depends on the particle sizes, granulator configuration, particle flow patterns and operating conditions. The second issue has been intensively

Table 1
A summary of proposed coalescence Kernels in the literature

Kernel	References
$\beta = \beta_0$	Kapur and Fuerstenau (1969)
$\beta = \beta_0 \frac{(u+v)^a}{(uv)^b}$	Kapur (1972)
$\beta = \beta_0 \frac{(u^{2/3}+v^{2/3})}{1/u+1/v}$	Sastry (1975)
$\beta = a(u+v)$	Golovin (1963)
$\beta = a\frac{(u-v)^2}{(u+v)}$	Golovin (1963)
$\beta = \begin{cases} k, t < t_s \\ a(u+v), t > t_s \end{cases}$ k: constant, t_s: switching time	Adetayo et al. (1995)
$\beta = \begin{cases} k, w < w^* \\ 0, w > w^* \end{cases}$ $w = \frac{(u+v)^a}{(uv)^b}$ k, a, b: constants w^*: critical granule volume	Adetayo and Ennis (1997)
$\beta = \beta_0(1/u + 1/v)^{1/2}(u^{1/3}+v^{1/3})^2$ $\beta = \beta_0(u^{-1/3} + v^{-1/3})(u^{1/3}+v^{1/3})$	Friedlander (1977, 2000)
$\beta\vert_{u,v} = \begin{cases} \beta_1 \; \textit{Types I \& II without permanent deformation} \\ \beta_2 \; \textit{Type II with permanent deformation} \\ 0 \; \textit{rebound} \end{cases}$	Liu and Litster (2002)

studied by Liu et al. (2000) with the identification of the following most important aspects affecting the success of coalescence: elastic–plastic properties, viscous fluid layer, head of collision, and energy balance. The authors have also observed that there are two types of coalescences distinguished by particle deformations. The Type I coalescence is not associated with any particle deformation during the collision, whereas the Type II coalescence is accompanied by particle deformations. Liu and Litster (2002) further proposed a new physically based coalescence kernel model based on the criteria developed earlier (Liu et al., 2000). From these fundamental studies, it can be determined qualitatively that the coalescence kernels should depend on particle sizes, energy consumptions, particle deformability, and most importantly, the moisture content (viscous fluid layer). A historical summary of proposed coalescence kernels is given in Table 1, which is an extension of the table originally presented by Ennis and Litster (1997) with the new coalescence kernel developed by Liu and Litster (2002) and another kernel from aerosol dynamics (Friedlander, 2000).

2.5. Two-dimensional (2-D) population balance models

We consider a perfect mixing, batch granulation system with two internal (property) coordinates: particle total volume v and liquid volume v_L. Because of the perfect mixing feature, there is no spatial coordinate in the model. However, the modelling strategy can be extended to continuous processes with both internal and external coordinates.

The 2-D population balance equation for a batch granulation process is

$$
\begin{aligned}
\frac{\partial}{\partial t} &f(v, v_L, t) \\
&= -\frac{\partial}{\partial v}\left[\frac{dv}{dt} f(v, v_L, t)\right] \\
&\quad - \frac{\partial}{\partial v_L}\left[\frac{dv_L}{dt} f(v, v_L, t)\right] \\
&\quad + \frac{1}{2}\int_0^v \int_0^{\min(v_L, v-v')} \beta(v - v', v_L - v'_L, v', v'_L) \\
&\quad \times f(v - v', v_L - v'_L, t) f(v', v'_L, t)\, dv'_L\, dv' \\
&\quad - f(v, v_L, t)\int_0^\infty \int_0^{v_L} \beta(v, v_L, v', v'_L) \\
&\quad \times f(v', v'_L, t)\, dv'_L\, dv'.
\end{aligned}
\tag{2.15}
$$

The relationship between the bi-variant number density function f and single-variant number density function n is determined as:

$$
n(v, t) = \int_0^v f(v, v_L, t)\, dv_L.
\tag{2.16}
$$

For the aggregation-only processes, the first two terms on the right hand side of Eq. (2.15) representing convective particle transport and particle growth by layering are negligible.
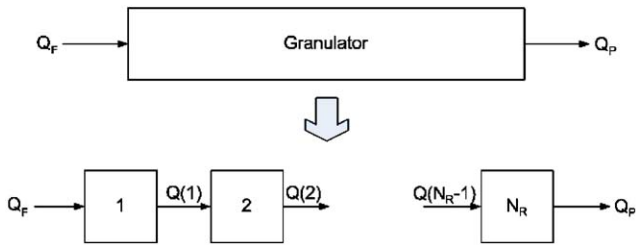
Fig. 3. Concept of lumped regions in series.

Eq. (2.15) is reduced to

$$\frac{\partial}{\partial t} f(v, v_L, t)$$

$$= +\frac{1}{2} \int_0^v \int_0^{\min(v_L, v-v')} \beta(v - v', v_L - v'_L, v', v'_L)$$
$$\times f(v - v', v_L - v'_L, t) f(v', v'_L, t) \, dv'_L \, dv'$$
$$- f(v, v_L, t) \int_0^\infty \int_0^{v_L} \beta(v, v_L, v', v'_L)$$
$$\times f(v', v'_L, t) \, dv'_L \, dv'. \qquad (2.17)$$

Under certain mathematical assumptions, a two-dimensional population balance equation can be reduced to two single dimension population balance equations, which will be described in the next section.

2.6. Reduced order models

2.6.1. Reduced order models using the concept of lumped regions in series

When particle populations are spatial dependent, such as that in a long rotating drum granulator, the population balance model is described by Eq. (2.13) with spatial variable z included in the model equation. In many industrial applications, the concept of lumped regions in series is used to reduce the model order. By using this method, a whole granulator is divided into a number of sections with an assumption that perfect mixing can be achieved in each section. The basic idea is schematically depicted in Fig. 3.

In Fig. 3, Q denotes the number flow-rate, the subscripts F and P represent the feed and product streams, respectively, and N_R is the total number of regions used to approximate the granulator. The reduced order model for Eq. (2.13) using the method of lumped regions in series is given by

$$\frac{\partial}{\partial t} n(v, i, t)$$

$$= -\frac{\partial}{\partial v} [G_i n(v, i, t)] + Q(i-1) \frac{n(v, i-1, t)}{n_t(i-1, t)}$$
$$- Q(i) \frac{n(v, i, t)}{n_t(i, t)} + \frac{1}{2} \int_0^v \beta(v - v', v') n(v - v', i, t)$$
$$\times n(v', i, t) \, dv' - n(v, i, t) \int_0^\infty \beta(v, v') n(v', i, t) \, dv',$$
$$i = 1, 2, \ldots, N_R, \qquad (2.18)$$

where i represents the ith region, n_t is the total number density, and $Q(0) = Q_F$.

2.6.2. Model order reduction for multi-dimensional population balances

Hounslow et al. (2001) and Biggs et al. (2003) have developed the concept of binder size distribution (BSD) to correlate moisture content with particle size. Based on BSD, the mass of binder in the size range $(v, v + dv)$ is quantified as $dM = M(v) \, dv$ and:

$$M(t, v) = \rho_L \int_0^v v_L f(v, v_L, t) \, dv_L. \qquad (2.19)$$

If the assumption that at a given size all granules have the same liquid content, the 2-D population balance equation given by Eq. (2.17) can be reduced to a set of two, one dimensional equations described as follows:

$$\frac{\partial}{\partial t} n(v, t) = \frac{1}{2} \int_0^v \beta(v - v', v') n(v - v', t) n(v', t) \, dv'$$
$$- n(v, t) \int_0^\infty \beta(v, v') n(v', t) \, dv, \qquad (2.20)$$

$$\frac{\partial}{\partial t} M(v, t) = \frac{1}{2} \int_0^v \beta(v - v', v') M(v - v', t) n(v', t) \, dv'$$
$$- M(v, t) \int_0^\infty \beta(v, v') n(v', t) \, dv. \qquad (2.21)$$

In their experiments, pharmaceutical materials were granulated in a high-shear mixer. Good agreement between experimental and simulation results were achieved enabling the granulation rates to be defined by two parameters: the critical binder volume fraction and the aggregation rate constant.

2.6.3. Reduced order models using the method of moments

The moments are defined as

$$M_j = \int_0^\infty v^j n(v) \, dv,$$
$$\mu_j = M_j / M_0,$$
$$j = 0, 1, 2, \ldots. \qquad (2.22)$$

Because of the variety of coalescence kernels, it is impossible to develop a generalised structure for reduced order models using the method of moments. A special kernel model is assumed in this work. The methodology can be extended to the development of moment models with different kernel structures. The example kernel model is assumed as:

$$\beta(v, v') = \beta_0 \frac{v^b + v'^b}{(vv')^a} = \beta_0 \left[\frac{v'^{(b-a)}}{v^a} + \frac{v^{(b-a)}}{v'^a} \right]. \qquad (2.23)$$

The discretised format of Eq. (2.23) is given by

$$\beta_{i,j} = \beta_0 \left[\frac{v_j^{(b-a)}}{v_i^a} + \frac{v_i^{(b-a)}}{v_j^a} \right]. \qquad (2.24)$$

The one-dimensional aggregation-only population balance equation described by Eq. (2.20) with the kernel model given

by Eq. (2.24) can be reduced to a set of ordinary differential equations as follows:

$$\frac{d}{dt} M_0 = -\beta_0 (\mu_{(b-a)} \mu_{-a}) M_0,$$

$$\frac{d}{dt} M_1 = 0,$$

$$\frac{d}{dt} M_r = \frac{1}{2} \beta_0 \sum_{k=1}^{r-1} \binom{r}{k} [\mu_{(k-a)} \mu_{(r-k+b-a)}$$
$$+ \mu_{(k+b-a)} \mu_{(r-k-a)}] M_0^2, \quad r = 2, 3, \dots, \quad (2.25)$$

where μ is defined in Eq. (2.22), for example, $\mu_{(k-a)} = M_{(k-a)}/M_0$. Eq. (2.25) involves the determination of fractional and negative moments. If the type of particle size distribution is more or less known, such as log-normal or Γ-distribution, Eq. (2.25) is solvable with the incorporation of interpolation and extrapolation techniques. For more general solution techniques, fractional calculus enabling the computation of fractional differentiations and integrations should be used.

2.7. Recent advances in higher dimensional models and mechanistic coalescence kernels

In consonance with the above study on two-dimensional population balance models, Iveson (2002) has suggested recently that a one-dimensional population balance model based on particle size is quite inadequate in accounting for the granulation process. As laid out previously, the three major contributing phenomena that have been identified in recent times in the granulation processes are wetting and nucleation; aggregation, layering and consolidation; breakage and attrition. Among these the major role played by consolidation is to reduce the porosity of the granules and thereby increase the fractional binder content and the chances of successful aggregation. The rate of aggregation itself is determined by both the size of the granules and its fractional binder content. Thus, at the least, the characterisation of the binder content and porosity in addition to the granule size is important in the granulation processes. Iveson (2002) also points out the importance of the heterogeneity at the macroscopic level in terms of binder distribution as well as size segregation effects that are required to be accounted for in a rigorous model of the granulation operation. He also points out that several applications also require the explicit characterisation of the concentration of the granules.

$$\frac{\partial n(m, \varepsilon, w, x, t)}{\partial t}$$
$$= B_{\text{coal}}(m, \varepsilon, w, x, t) - D_{\text{coal}}(m, \varepsilon, w, x, t)$$
$$+ C(m, \varepsilon, w, x, t) + W(m, \varepsilon, w, x, t), \quad (2.26)$$

wherein m is the total mass of the granule particle, ε is the particle porosity, w is the fractional binder content (fraction of binder to solid mass), and x is the composition of the solid (drug vs. excepient). The terms $B_{\text{coal}}(m, \varepsilon, w, x, t)$ and $D_{\text{coal}}(m, \varepsilon, w, x, t)$ account, respectively, for the birth and death of particles due to coalescence events. C accounts for consolidation and W accounts for wetting.

A similar multi-dimensional population balance model was also proposed by Verkoeijen et al. (2002). They extend the Iveson proposal in that they suggest the use of truly mutually independent particle properties as the internal variables. Thus, in a three-dimensional formulation, they propose the use of the volume of solid, volume of liquid and volume of gas as the internal coordinates (rather than the particle total volume, binder content and porosity which are not mutually independent of each other). This approach results in elegantly separating the underlying mesoscopic processes of aggregation, consolidation, breakage, drying and layering.

Immanuel and Doyle III (2004) propose the following multi-dimensional formulation of the population balance model for the granulation process, using the individual volumes of solid, liquid and air as the internal coordinates:

$$\frac{\partial}{\partial t} F(s, l, g, t) + \frac{\partial}{\partial g} \left(F(s, l, g, t) \frac{dg}{dt} \right)$$
$$+ \frac{\partial}{\partial s} \left(F(s, l, g, t) \frac{ds}{dt} \right) + \frac{\partial}{\partial l} \left(F(s, l, g, t) \frac{dl}{dt} \right)$$
$$= \Re_{\text{aggre}}(s, l, g, t) + \Re_{\text{break}}(s, l, g, t)$$
$$+ \Re_{\text{nuc}}(s, l, g, t), \quad (2.27)$$

where $F(s, l, g, t)$ is the population density function, defined such that $F(s, l, g, t) \, ds \, dl \, dg$ is the moles of granules of solid volume between s and $s + ds$, liquid volume between l and $l + dl$, and gas volume between g and $g + dg$. $\Re_{\text{nuc}}(s, l, g, t)$ accounts for the rate of nucleation of new granules. $\Re_{\text{aggre}}(s, l, g, t)$ accounts for the gain/loss of granules due to the aggregation process, while $\Re_{\text{break}}(s, l, g, t)$ comprises similar terms due to granule breakage. The partial derivative with respect to g on the left hand side accounts for the consolidation phenomenon, wherein dg/dt is negative (there is a continuous decrease in the pore volume of the granules as they compact, while the solid and liquid content of each granule is left unaltered). Likewise, the partial derivative term with respect to s accounts for any simultaneous crystallisation and the layering of the granule surface with the solid, while the term with respect to l accounts for any drying effects. These latter two terms are usually restricted to certain special cases of granulation applications.

The rate processes of aggregation, consolidation, breakage and nucleation that underlie the granulation process have been well-characterised over the years, as borne out by an exhaustive review by Iveson et al. (2001). The various mesoscale processes have been characterised in terms of dimensionless parameters and regime charts have been developed. Although some of the kernels shown in Table 1 are physically based and inspired by the underlying process mechanisms, they are not truly mechanistic.

Immanuel and Doyle III (2004) and Immanuel et al. (2004) have recently attempted the derivation of mechanistic

kernels for the processes, mainly the aggregation process. The mechanistic modelling of the aggregation kernels requires the identification of the net attraction potentials (energies) between the different particle pairs. In the granulation process, the kinetic energy of the particles constitutes the major potential of attraction between the granules $((1/2)mu_0^2)$ (Ennis et al., 1991; Liu et al., 2000; Iveson et al., 2001). The dissipation of the kinetic energy of the granules is primarily attributed to the viscous forces in the liquid binder film. Other forces that contribute to the dissipation are the collision energy and the elastic energy of the granules, which come into play only when the particles are involved in an actual collision by overcoming the viscous dissipation. Different forces become important in different regimes of particle sizes, binder content and operating conditions (mixing rates). The capillary repulsive forces between the particles are usually neglected in relation to the stronger viscous forces.

The particles that collide with each other as a result of their kinetic energy will either coalesce or rebound. Coalescence is classified into two types—types I and II. Type I coalescence occurs when the viscous force is able to overcome the kinetic energy, causing the particles to coalesce before the occurrence of a collision (through the liquid bridge). Type II coalescence occurs when the particles actually collide and loose all the kinetic energy. The elastic energy causes the particles to rebound, being dissipated again in the viscous binder layer. If this dissipation is complete, then coalescence occurs (either with or without complete recovery of the deformation). See Iveson et al. (2001) for further mechanistic details.

Net attractive potential for type I coalescence (balancing the kinetic energy with the viscous repulsion) is given by Eq. (2.28), where p_1 and p_2 are the two particles, m is the reduced mass of the particles, h is the separation distance between the particles, and u is the varying relative velocity of the particles as they approach each other. The velocity u is also defined in Eq. (2.28), wherein h_0 is the depth of the liquid binder film on the surface, u_0 is the initial approach velocity of the particles (based on the mixing rates in the granulator), and St_v is the viscous Stokes number.

$$\Psi(p_1, p_2, h) = \tfrac{1}{2}m(2u(h))^2,$$

$$u = u_0 \quad \text{for } h > h_0$$
$$= u_0 \left(1 - \frac{1}{St_v} \ln\left(\frac{h_0}{h}\right)\right) \quad \text{for } h < h_0. \tag{2.28}$$

For type II coalescence, two different sequential processes are involved—the forward and the reverse paths. The process with the higher energetics is the rate-determining process. The net attractive potential for the two processes are defined in Eqs. (2.29), where E_c is the energy lost during impact and deformation, u_1 being the velocity at impact. In this equation, u' is the net rebound velocity and δ'' is the

permanent plastic deformation in the granules.

$$\Psi_{\text{forward}}(p_1, p_2, h) = \tfrac{1}{2}m(2u(h))^2 - E_c,$$

$$\Psi_{\text{reverse}}(p_1, p_2, h) = -\tfrac{1}{2}m(2u'(h))^2,$$

$$E_c = \tfrac{1}{2}m(2u_1)^2,$$

$$u'(h) = u_2 - \frac{3\pi\mu\tilde{D}^2}{16\tilde{m}h^2}\left[(\delta'')^2\left(\frac{h^2}{h_a^2} - 1\right)\right.$$
$$\left. + 2h\delta''\left(\frac{h}{h_a} - 1\right) + 2h^2 \ln\left(\frac{h}{h_a}\right)\right]$$
$$\qquad \text{for } 0 < h < h_0$$
$$= u'(h_0) \quad \text{for } h > h_0, \tag{2.29}$$

$$\delta'' = \left(\frac{8}{3\pi}\right)^{1/2} St_{\text{def}}^{1/2} \tilde{D}\left[1 - \frac{1}{St_v}\ln\left(\frac{h_0}{h_a}\right)\right]$$
$$\times \left[1 - 7.36\frac{Y_d}{E^*}St_{\text{def}}^{1/2}\right]\left[1 - \frac{1}{St_v}\ln\left(\frac{h_0}{h_a}\right)\right]^{-1/2}.$$

These steady state forces can be incorporated into a dynamic calculation of the aggregation rates and the aggregation kernel, as described in the emulsion polymerisation literature (Immanuel et al., 2003). This net attractive potential information can be employed in the Smoluchowski formulation as shown in Eq. (2.30). The Fuch Stability ratio W is defined in Eq. (2.31) for types I and II aggregation, respectively. In these equations, r_i is the radius of particle p_i, k is the Boltzmann constant, T is the temperature, and c_1 is an adjustable constant.

$$\beta(p_1, p_2) = c_1 \frac{4\pi u_0(r_1 + r_2)^2}{W} \tag{2.30}$$

$$W(p_1, p_2)$$
$$= (r_1 + r_2)\int_{D=r_1+r_2}^{\infty} \frac{e^{\psi(p_1, p_2, D)/kT}}{D^2}\, dD \tag{2.31}$$

$$\frac{W(p_1, p_2)}{r_1 + r_2}$$
$$= \max\left(\int_{D=r_1+r_2}^{\infty} \frac{e^{-\psi_{\text{forward}}(p_1, p_2, D-r_1-r_2)/kT}}{D^2}\, dD,\right.$$
$$\left. \times \int_{D=r_1+r_2}^{\infty} \frac{e^{-\psi_{\text{reverse}}(p_1, p_2, D-r_1-r_2)/kT}}{D^2}\, dD\right).$$

2.8. Discrete particle simulation approaches to granulation modelling

Gantt and Gatzke (2005) propose a discrete element simulation method in implementing the population balance. In this strategy, the population balance equation itself is not directly involved. Instead, the underlying particle rate processes (aggregation, consolidation, breakage) are directly simulated. A sample of particles within the control volume of the granulator is considered, and the initial conditions

such as positions in a 3-D space, velocities in the three directions, internal stresses, etc. are assigned for each particle. The particle rate processes are simulated, and hence their internal coordinates are updated directly.

The advantage with this approach is that this strategy overcomes the hurdles with the solution of the rigorous population balance models. An additional advantage is that they enable accounting for the underlying problem physics in a straightforward manner, in contrast to the derivation of the kernels employing strategies such as those employed by Immanuel and Doyle III (2004) and Immanuel et al. (2004). Further, these mechanistic kernels are computationally intensive, although in a three-dimensional formulation of the population balance, the kernels are time-invariant and hence need to be computed only once. An alternative strategy is to directly incorporate these mechanistic understandings through discrete element simulation methods. In their study, Gantt and Gatzke (2005) directly simulate the underlying mechanisms in determining the variations of the particle porosities; in determining the chances of successful aggregation; and in determining the attainment of the critical stress levels that lead to particle breakage. They consider the volume distribution of a volume-based population, along the lines of Verkoeijen et al. (2002), in simulating the processes of consolidation, aggregation and breakage of seeded granulation in their study, with a semi-empirical characterisation of each of these processes.

Although the discrete element method (DEM) has been used for the modelling of granular flows for some time (see, e.g., Hoomans (1999) for an excellent review), it has only been adopted for the modelling of granulation processes relatively recently. Khan (1998) used DEM-based simulations for the modelling of granulation and granule break-up in a shear flow, while Goldschmidt (2001) performed detailed DEM simulations of a top-spray fluidised bed granulation process.

The discrete element method is based on the same principles as molecular dynamics (MD) simulation. That is the Newton's law of motion is simultaneously solved for a large number of particles either in a computational unit cell with periodic boundaries or on a computational domain representing the entire process vessel or its subset. In general, the following equations are solved:

$$m_i \frac{d\mathbf{u}_i}{dt} = \mathbf{F}_i \tag{2.32}$$

and

$$I_i \frac{d\boldsymbol{\omega}_i}{dt} = \mathbf{M}_i, \tag{2.33}$$

where m_i is particle mass, $\mathbf{u}_i$ is velocity, t is time, I_i is moment of inertia, $\boldsymbol{\omega}_i$ is angular velocity, $\mathbf{M}_i$ is the net torque, and $\mathbf{F}_i$ is the net force acting on particle i. The net force is usually written as the sum of three contributions:

$$\mathbf{F}_i = \mathbf{F}_i^H + \mathbf{F}_i^P + \mathbf{F}_i^E, \tag{2.34}$$

where $\mathbf{F}^H$ is force due to fluid–particle interactions (drag force), $\mathbf{F}^P$ is force due to particle–particle interactions (during collisions), and $\mathbf{F}^E$ is a force acting on the particle due to an external field (e.g. gravitational). The main differences between various implementations of DEM are in the nature of the particle–particle interactions (hard-sphere model, inelastic collisions, etc.) and in the way fluid–particle coupling is treated. For example $\mathbf{F}^H$ is sometimes ignored altogether, on the other hand the full Navier–Stokes equations for the continuum fluid phase can be solved simultaneously with the discrete particle motion.

When DEM is used for the modelling of agglomeration, the inter-particle force model must allow for the formation of reversible or irreversible particle–particle bonds, and criteria for agglomeration must be defined. A commonly used inter-particle contact model is based on the linear spring–dashpot model for the normal component of inter-particle contact, with friction for the tangential component (e.g., Subero et al., 1999). To allow for inter-particle bond formation, a surface energy term is introduced. The bond strength between two particles is then simply the surface energy times the contact area. Such inter-particle bond models are suitable especially for the modelling of phenomena such as impact breakage of pre-existing agglomerate, which undergo brittle failure (Thornton et al., 1999). In wet granulation the inter-particle bonds are primarily due to capillary bridges. This situation has been considered e.g. by Lian et al. (1998), who used the viscous force due to an axially stretched capillary bridge as the inter-particle force when simulating the coalescence of wet agglomerates.

An important implementation detail, when using DEM for granulation modelling, is the representation of agglomerates. Two approaches have been used. The discrete elements can either strictly represent primary particles, which maintain their identity even as they become part of larger agglomerates, or both primary particles and agglomerates are represented by discrete elements, in which case the identities of elements that have coalesced are lost and a new, larger discrete element is created in their place. The former approach has been used by Tardos et al. (1997). Its advantage is that further deformation or breakage of the agglomerates can be simulated, and that information about the granule morphology is obtained automatically from the simulation. The main disadvantage is computational cost. The latter approach has been used by Goldschmidt et al. (2003). When two discrete elements coalesce, they lose their identity and a new discrete element is created. Its diameter and composition are calculated from those of the parent particles by applying a mass balance but additional assumptions have to be made when calculating properties such as porosity or surface coverage, which are generally not conserved after coalescence. The main advantage of this approach is that large systems can be simulated. The disadvantage is that no information about the agglomerate morphology is generated and the possibility of agglomerate breakage is not implicit in the simulation.

Talu et al. (2000) considered a mixture of dry and wet particles in a two-dimensional shear flow. The simulations yielded asymptotic particle size distributions as function of the Stokes number, the Capillary numbers, and the thickness of binder layer on the wet particles. Importantly, the distributions of granule shape (called "compactness") were also obtained from the simulations. Khan and Tardos (1997) also investigated a closely related problem—that of stability of existing wet agglomerate in a shear flow. Expressions for the critical Stokes number, which allow the estimation of the maximum granule size that can exist in a given shear field, have been derived from the simulations.

Goldschmidt et al. (2003) modelled top-spray fluidised bed granulation by DEM coupled with a detailed hydrodynamic model of the fluid phase. A two-dimensional situation was considered. Binder droplets and solid particles were explicitly accounted for in the DEM simulation, and criteria for the occurrence of coalescence as function of the fractional liquid coverage of the colliding particles have been applied. The solidification of binder has also been modelled. The simulations gave the size and composition distributions of the resulting granules. The influence of several parameters on granulation kinetics has been investigated, including binder spray rate, droplet size, fluidisation velocity, and the minimum thickness of binder layer assumed to be present on the particles once wetted.

By default the particles in a DEM simulation are considered to be spherical but extensions to non-spherical particles also exist. One possibility is to use truly non-spherical discrete elements, as was done by Hogue (1998), or to approximate the shape of non-spherical particles by fixed assemblies formed from spherical ones, as suggested by Abou-Chakra et al. (2004). DEM modelling of granulation has so far been restricted to spherical discrete elements. Although DEM simulation can yield both size and composition distribution of granules, it is generally not suitable for realistic representation of granule microstructure (i.e., the internal distribution of primary solids, binder, and porosity in the granule). Microstructure is an important granule attribute, as it determines among other things the release rate of an active ingredient from the granule (Stepanek, 2004). Stepanek and Warren (2002) have used the volume-of-fluid (VoF) method to generate granule microstructures by direct numerical simulation of primary particle packing, binder droplet spreading, and binder solidification.

3. Solving and using population balances

3.1. Hounslow discretization method

Hounslow et al. (1988) developed a relatively simple discretisation method by employing a M–I approach (the Mean value theorem on frequency). The population balance equations, such as Eq. (2.20), are normally developed using particle volume as the internal coordinate. Because of the

identified advantages of length-based models, Hounslow et al. (1988) performed the coordinate transformation to convert the volume-based model described by equation (2.20) to a length-based model as follows:

$$
\begin{aligned}
\frac{\mathrm{d}}{\mathrm{d}t} &\, n(L, t) \\
&= \frac{L^2}{2} \int_0^L \\
&\quad \times \frac{\beta \lfloor (L^3 - \lambda^3)^{1/3}, \lambda \rfloor n \lfloor (L^3 - \lambda^3)^{1/3}, t \rfloor n(\lambda, t)}{(L^3 - \lambda^3)^{2/3}} \, \mathrm{d}\lambda \\
&\quad - n(L, t) \int_0^\infty \beta(L, \lambda) n(\lambda, t) \, \mathrm{d}\lambda
\end{aligned}
\tag{3.1}
$$

in which L and λ denote the characteristic length of particles. The Hounslow method is based on a geometric discretisation with the following ratio between two successive size intervals:

$$
L_{i+1}/L_i = \sqrt[3]{2}, \text{ or } v_{i+1}/v_i = 2,
\tag{3.2}
$$

where L and v represent the characteristic length and volume of particles, respectively, the subscripts $i + 1$ and i denote the size classes. The population balance equation for coalescence only granulation processes described by Eq. (2.20) is converted into a set of discretised population balance equations in various size intervals by using this technique. That is, the change of number density in the ith size interval is given by

$$
\begin{aligned}
\frac{\mathrm{d}}{\mathrm{d}t} n_i &= n_{i-1} \sum_{j=1}^{i-2} (2^{j-i+1} \beta_{i-1,j} n_j) + \frac{i}{2} \beta_{i-1,i-1} n_{i-1}^2 \\
&\quad - n_i \sum_{j=1}^{i-1} (2^{j-i} \beta_{i,j} n_j) - n_i \sum_{j=1}^{i_{\max}} (\beta_{i,j} n_j), \\
&\qquad i = 1, 2, \ldots, i_{\max}.
\end{aligned}
\tag{3.3}
$$

The binder size distribution model described by Eq. (2.21) can also be discretised using a similar numerical scheme as follows (Biggs et al., 2003):

$$
\begin{aligned}
\frac{\mathrm{d}}{\mathrm{d}t} M_i &= M_{i-1} \sum_{j=1}^{i-2} (2^{j-i+1} \beta_{i-1,j} n_j) \\
&\quad + n_{i-1} \sum_{j=1}^{i-2} (2^{j-i+1} \beta_{i-1,j} n_j) \\
&\quad + n_i \sum_{j=1}^{i-1} [(1 - 2^{j-i}) \beta_{i,j} M_j] + \beta_{i-1,i-1} n_{i-1} M_{i-1} \\
&\quad - M_i \sum_{j=1}^{i-1} (2^{j-i} n_j) - M_i \sum_{j=1}^{i_{\max}} (\beta_{i,j} n_j), \\
&\qquad i = 1, 2, \ldots, i_{\max}.
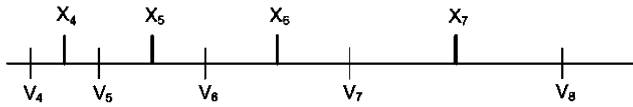\end{aligned}
\tag{3.4}
$$

Fig. 4. General grid used with Kumar and Ramkrishna numerical technique.

3.2. Kumar and Ramkrishna's discretisation technique

Kumar and Ramkrishna (1996) developed a discretisation method by using a grid with a more general and flexible pattern with fine or coarse discretisations in different size ranges. The size range between two sizes v_i and v_{i+1} is called the ith section, and the particle size in this section is simply denoted by x_i (grid point) such that $v_i < x_i < v_{i+1}$ as seen in Fig. 4.

A particle of size v in the size range x_i and x_{i+1} can be represented by two fractions $a(v, x_i)$ and $b(v, x_{i+1})$ associated with the two grid points x_i and x_{i+1}, respectively. For the conservation of two general properties $f_1(v)$ and $f_2(v)$, these fractions satisfy the following equations:

$$a(v, x_i) f_1(x_i) + b(v, x_{i+1}) f_1(x_{i+1}) = f_1(v),$$
$$a(v, x_i) f_2(x_i) + b(v, x_{i+1}) f_2(x_{i+1}) = f_2(v). \quad (3.5)$$

By using this composition technique for particle properties, discrete equations for coalescence-only population balance model given be Eq. (2.20) have been formulated as follows:

$$\frac{\mathrm{d}n_i}{\mathrm{d}t} = \sum_{\substack{j,k \\ x_{i-1} \leqslant (x_j + x_k) \leqslant x_{i+1}}}^{j \geqslant k} \left(1 - \frac{1}{2}\delta_{j,k}\right)\eta\beta(j,k)n_j(t)n_k(t)$$
$$- n_i(t) \sum_{k=1}^{i_{\max}} \beta(i,k)n_k(t). \quad (3.6)$$

In Eq. (3.6), n_i, β, $i_{\max}$ are defined previously, $\delta_{j,k}$ is the Dirac-delta function, and η is defined as follows:

$$\eta = \frac{x_{i+1} - v}{x_{i+1} - x_i}, \quad x_i \leqslant v \leqslant x_{i+1},$$
$$\eta = \frac{v - x_{i-1}}{x_i - x_{i-1}}, \quad x_{i-1} \leqslant v \leqslant x_i. \quad (3.7)$$

The first and second terms on the right hand side of Eq. (3.6), respectively, represent the birth rate and death rate of particles in the ith size interval due to coalescence.

Attention should be paid to the selection of the internal coordinates. The original Kumar–Ramkrishna discretisation should be applied to volume-based models rather than length-based models. Although both are inter-convertible, it is important to check the consistency in numerical computations.

3.3. Wavelet based methods

The wavelet-based methods are relatively new numerical schemes for solving population balance equations consisting of both differential and integral functions (Liu and Cameron, 2001). Again, the volume-based population balance equations with particle volume as the internal coordinate are used to demonstrate the main characteristics of the wavelet methods. The most important advantage of these methods over other numerical techniques is their ability to effectively deal with steep moving profiles. In this section, only the basic algorithms of the wavelet collocation method for practical applications using the Daubechies wavelets are discussed.

Similar to other collocation methods, the coordinates should be normalised within the interval [0, 1]. For the 1-D population balance equation given by Eq. (2.11), this can be done by introducing the linear transformation $x = v/v_{\max}$, where x is the dimensionless particle volume and $v_{\max}$ is the maximum particle size in the system. The original integral intervals $[0, v]$ and $[0, \infty]$ are transformed to $[0, x]$ and $[0, 1]$, respectively. Consequently, Eq. (2.11) becomes

$$\frac{\partial}{\partial t} n(x, t) = -\frac{\partial}{\partial x}[G(x)n(x, t)]$$
$$+ \frac{v_{\max}}{2} \int_0^x \beta(x - x', x')n(x - x', t)$$
$$\times n(x', t)\,\mathrm{d}x' - v_{\max}n(x, t)$$
$$\times \int_0^1 \beta(x, x')n(x', t)\,\mathrm{d}x', \quad (3.8)$$

where $G(x)$ is defined as $\mathrm{d}x/\mathrm{d}t$ rather than $\mathrm{d}v/\mathrm{d}t$. For a broad class of engineering problems, the approximate solution of a general function $w(x)$ with J-level resolution can be written in terms of its values in the dyadic points:

$$w_J(x) \approx \sum_m w_J(2^{-J}m)\theta(2^J x - m), \quad (3.9)$$

where $\theta(x)$ is denoted as the autocorrelation function of scaling function. We first solve the coalescence only PBE with $G(x) = 0$. If a J-level wavelet method is used, the matrix representation at the ith dyadic point is given by:

$$\frac{\partial n_i}{\partial t} = \frac{v_{\max}}{2}[n_0 \ n_1 \ \cdots \ n_{2^J}]\mathbf{M}^{3,i}$$
$$\times \begin{bmatrix} n_0 \\ n_1 \\ \vdots \\ n_{2^J} \end{bmatrix} - v_{\max}n_i\mathbf{M}_i^2 \begin{bmatrix} n_0 \\ n_1 \\ \vdots \\ n_{2^J} \end{bmatrix}, \quad (3.10)$$

where n_i is the number density at the ith dyadic (collocation) point. The operational matrix $\mathbf{M}^{3,i}$ and vector $\mathbf{M}_i^2$ are constructed as follows. $\mathbf{M}^{3,i}$ are $(2^J + 1) \times (2^J + 1)$ operational matrices at volume points i represented as

$$\mathbf{M}^{3,i} = \begin{bmatrix} M_{0,0}^{3,i} & M_{0,1}^{3,i} & \cdots & M_{0,2^J}^{3,i} \\ M_{1,0}^{3,i} & M_{1,1}^{3,i} & \cdots & M_{1,2^J}^{3,i} \\ \vdots & \vdots & \ddots & \vdots \\ M_{2^J,0}^{3,i} & M_{2^J,1}^{3,i} & \cdots & M_{2^J,2^J}^{3,i} \end{bmatrix}, \quad (3.11)$$

$\mathbf{M}_i^2$ are $1 \times (2^J + 1)$ operational vectors at volume points i described by

$$\mathbf{M}_i^2 = [M_{i,0}^2 \; M_{i,1}^2 \; \cdots \; M_{i,2^J}^2].$$

The operational matrices $\mathbf{M}^{3,i}$ and $\mathbf{M}_i^2$, together with other needed matrices and functions at various resolution levels for wavelet based methods are available at URL: http://www.cheque.uq.edu.au/psdc.

3.4. Monte Carlo methods

There is a long history in studies on the application of Monte Carlo methods to process engineering. The first serious research paper on a Monte Carlo treatment for systems involving population balances could be credited to Spielman and Levenspiel (1965). Since then, a significant number of publications have appeared in the literature on the resolution of population balance equations using Monte Carlo methods (Ramkrishna, 2000). Comprehensive Monte Carlo treatments are described in the literature (e.g. Ramkrishna, 2000; Kaye, 1997). Only selected issues on basic techniques will be addressed.

3.4.1. Classification of Monte Carlo methods
Monte Carlo methods can be used in two ways:

1. Direct evaluation of difficult functions. For example, the integral given by

$$I = \int_a^b g(x)\,\mathrm{d}x \tag{3.12}$$

can be evaluated as

$$I = E(Y) = E[(b-a)g(X)] = E[\bar{Y}(n)]$$
$$\bar{Y}(n) = \cdots (b-a)\frac{\sum_{i=1}^n g(X_i)}{n}, \tag{3.13}$$

where $X_1, X_2, \ldots, X_n$ are random variables defined in the closed interval $[a, b]$, and $E(Y)$ denotes the mathematical estimation of function Y.

2. Artificial realization of the system behaviour (Ramkrishna, 2000). This method is commonly applied to complex particulate processes. In the artificial realization, the direct evaluation of integral and differential functions is replaced by the simulation of the stochastic behaviour modelled by using a randomness generator to vary the behaviour of the system (Kaye, 1997). The coalescence kernels for granulation processes, are still essential in Monte Carlo simulations.

Monte Carlo methods for the artificial realization of the system behaviour can be divided into time-driven and event driven simulations. In the former approach, the time interval Δt is chosen, and the realization of events within this time interval is determined stochastically. In the latter case, the time interval between two events is determined based on the rates of processes. In general, the coalescence rates in granulation processes can be extracted from the coalescence kernel models. The event-driven Monte Carlo can be further divided into constant volume methods in which the total volume of particles is conserved (Gooch and Hounslow, 1996), and constant number method in which the total number of particles in the simulation remains constant. The main advantage of the constant number method for granulation processes is identified as: the population remains large enough for accurate Monte Carlo simulations (Smith and Matsoukas, 1998; Wauters, 2001). An additional advantage associated with the constant number methods is its ability to reduce the re-numbering effort. Consequently, the constant number method is recommended.

3.4.2. Key equations for constant number Monte Carlo simulation
Key equations needed in Monte Carlo simulations include the inter-event time Δt_q representing the time spent from $q-1$ to q Monte Carlo steps, coalescence kernel K_{ij}, normalised probability p_{ij} for a successful collision between particles i and j, and a number of intermediate variables. The coalescence kernel can be divided into particle property independent part K_c and dependent part $k_{ij}(\mathbf{X}_i, \mathbf{X}_j)$ as follows:

$$K_{ij} = K_c k_{ij}(\mathbf{X}_i, \mathbf{X}_j),$$
$$i, j = 1, 2, \ldots, N, \tag{3.14}$$

where $\mathbf{X}$ denotes the vector of internal coordinates representing particle properties, such as size and moisture content, and N is the total number of particles in the simulation system. It can be seen that Eq. (3.14) is similar to the coalescence kernel given by $\beta_{ij} = \beta_0 k_{ij}(v_i, v_j)$ described in the previous sections for one-dimensional systems. However, it should be pointed out that i and j in Eq. (3.14) are used to identify the individual particles, whereas that in β_{ij}, $i, j = 1, 2, \ldots, i_{\max}$ are size classes rather than particle identity numbers. In order to avoid confusion, β_{ij} and β_0 are replaced by K_{ij} and K_c, respectively in Monte Carlo simulations. The normalised probability for successful collision is given by

$$p_{ij} = \frac{k_{ij}}{k_{\max}}, \tag{3.15}$$

where $k_{\max}$ is the maximum value of the coalescence kernel among all particles. The final result of the inter-event time is given by

$$\Delta t_q = \frac{2\tau_c}{\langle k_{ij}\rangle}\frac{1}{N}\left(\frac{N}{N-1}\right)^q \tag{3.16}$$

with

$$\tau_c = \frac{1}{K_c C_0} \tag{3.17}$$

and

$$\langle k_{ij}\rangle = \frac{\sum_{i=1}^N \sum_{j=1, i\neq j}^N k_{ij}}{N(N-1)}. \tag{3.18}$$

In Eq. (3.17), C_0 is the total number concentration at $t = 0$ defined by $C_0 = N/V_0$ where V_0 is the volume of particles at the initial time. Interested readers are referred to Smith and Matsoukas (1998) for detailed mathematical derivations.

Monte Carlo methods are applicable to both one-dimensional and multi-dimensional coalescence processes without any theoretical and algorithmic hurdles. However most reported results with good agreement with experimental data are limited to one-dimensional systems except that reported by Wauters (2001) and Goodson et al. (2004). This is mainly due to the lack of reliable multi-dimensional kernel models rather than the applicability of Monte Carlo methods.

Vikhansky and Kraft (2004) address the problem of the numerical calculation of parametric sensitivity for population balance models, which information could be used to solve the inverse problem of the identification of underlying kernel parameters from experimental data (for a known structural form of the kernel). The usual practice in performing sensitivity studies is to perform several numerical solutions at different values of the parameters, and employ a finite difference scheme to derive the parametric sensitivities. In their paper, a method is presented to simultaneously develop the parametric sensitivity along with the numerical solutions, *albeit* based on a time-driven Monte Carlo based solution technique.

According to their strategy, an exponentially distributed time increment based on a parameter $\hat{\pi}_{\alpha\beta}$ is employed. At each time step, a pair of particles (k, l) is chosen for collision based on the distribution $\hat{\pi}_{kl}/\sum_{\alpha=1,\beta=1}^{N} \hat{\pi}_{\alpha\beta}$. The probability of successful coalescence of the chosen particle pair is defined based on the chosen parameter $\hat{\pi}_{\alpha\beta}$ as $\pi_{kl}/\hat{\pi}_{kl}$, where $\pi_{kl}(\lambda) = K(x_k, x_l; \lambda)w_l/x_l$ where w_n is the total weight of particles of mass x_n (in discrete size interval n) and $K(x_k, x_l; \lambda)$ is the size-dependent coalescence kernel that is dependent on the parameter λ. Thus, the particle x_k is replaced by $x_k + x_l$ in the discrete sample, and the corresponding weights in the two size intervals (w_k and w_{k+l}) are updated. Thus, at each time instant, any distribution dependent property $H(t, m; \lambda)$ can be calculated as follows:

$$H(t, m; \lambda) \approx \sum_{n=1}^{N} w_n h(x_n). \tag{3.19}$$

The variation of the particle density with parameter λ is then updated as follows:

$$\frac{\partial m(t, m; \lambda)}{\partial \lambda} \approx \sum_{n=1}^{N} w_n W_n, \tag{3.20}$$

where W_n represents the sensitivities which are updated as follows: $W_k = W_k + W_l + \partial_\lambda \ln(K)$ if the coagulation is successful and $W_k = W_k - w_l K(\partial_\lambda \ln(K) + W_l)/(\hat{w}_l \hat{K} - w_l K)$ in the event of unsuccessful collision. See Vikhansky and Kraft (2004) for more details on the algorithm.
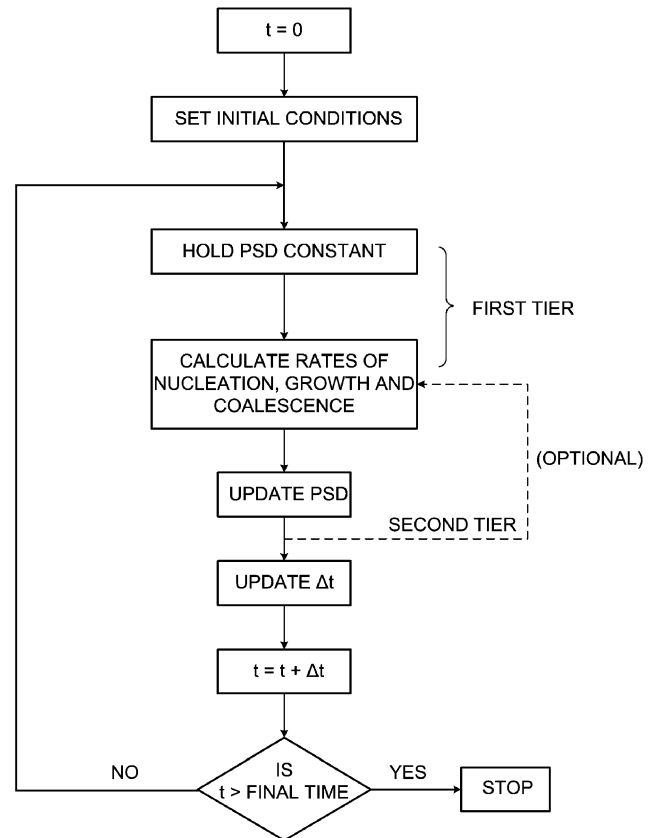

Fig. 5. Schematic of a hierarchical two-tier solution strategy for population balance models.

3.5. Other solution techniques

Another recent development in solution techniques has been presented by Immanuel and Doyle III (2003a). This technique is based on a finite-element discretisation of the particle population, and tracks the total particles within each of the bins. The equation representing the total particles within each bin is derived from the population balance equation in a straight-forward manner (partial analytical solution). The particle population in each bin is updated employing a hierarchical strategy, as depicted in Fig. 5. The individual rates of nucleation, growth and coalescence in each bin is computed in the first tier of the algorithm (at each time step), and the particle population is updated in the second tier. A simple predictor–corrector technique may be utilised for information exchange between the two tiers.

Employing the two-tier hierarchical solution strategy enables orders of magnitude improvement in the computation times. The improvement in computation times is achieved partly due to a reduction of the stiffness of the system of equations by a decomposition solution strategy for the nucleation, growth and coalescence models. In effect, the population balance equation is reformulated in terms of the individual growth, aggregation, nucleation and breakage events (as appropriate), thereby accommodating the

differences in their time scales. The other major factor that contributes to this improvement in computation time is the off-line analytical solution that is proposed for the aggregation quadratures. This results in casting the complex integrals in terms of simpler terms, major portions of which can be computed just once at the start, thereby leading to a substantial reduction in the computational load. These analytical solutions for the quadratures are derived based on an assumption of a uniform particle density within each element, although this assumption can be easily relaxed to enable larger finite elements. It also involves the assumption that the coalescence kernel for particles between any two bins is a constant (i.e., $\beta(V', V - V')$ in the following equation is constant for all particle coalescences between bins i and j).

$$
\begin{aligned}
\mathfrak{R}'_{\text{formation}}(V, t) \\
= \frac{1}{2V_{\text{aq}}} \int_{V=V_{j-1}}^{V_j} \left[\int_{V'=V_{\text{nuc}}}^{V-V_{\text{nuc}}} \beta(V', V - V') \right. \\
\left. \times F_V(V', t) F_V(V - V', t)\, \mathrm{d}V' \right] \mathrm{d}V.
\end{aligned}
\tag{3.21}
$$

See Immanuel and Doyle III (2003a) for the detailed analytical solutions.

Immanuel and Doyle III (2004) discuss the extension of the above 1-D algorithm to the multi-dimensional case. The ranges of volumes of solid, liquid and gas are divided into three-dimensional grids (finite volumes or the bins). In this case, the algorithm models the total particle count within each of these bins, defined such that $F_{i,j,k}$ is the total moles of particles within the (i, j, k)th bin. The layering effect and the drying effect (which account for the continuous change in the solid and liquid contents of the granules) are neglected in this case. Thus, continuous growth is restricted to the gas volume (due to consolidation). In the following equation, g_k is the lower boundary of gas volume in the kth bin along the gas volume, and ΔG_k is the width of the kth bin along the gas volume.

$$
\begin{aligned}
\frac{\mathrm{d}}{\mathrm{d}t} F_{i,j,k} + \left(\frac{F_{i,j,k}}{\Delta G_{i,j,k}} \right) \left. \frac{\mathrm{d}g}{\mathrm{d}t} \right|_k - \left(\frac{F_{i,j,k+1}}{\Delta G_{i,j,k+1}} \right) \left. \frac{\mathrm{d}g}{\mathrm{d}t} \right|_{k+1} \\
= \int_{s_{i-1}}^{s_i} \int_{l_{i-1}}^{l_i} \int_{g_{i-1}}^{g_i} \mathfrak{R}_{\text{aggre}}(s, l, g, t)\, \mathrm{d}s\, \mathrm{d}l\, \mathrm{d}g.
\end{aligned}
\tag{3.22}
$$

Extensions of the analytical solutions for the aggregation integrals to multi-dimensional cases is straightforward. The aggregation term in the equation above assumes a six-dimensional form in the current three-dimensional case ($\mathfrak{R}_{\text{aggre}}(s, l, g, t)$ itself being a three-dimensional integral). This six-dimensional integral can be re-cast as a multiple of three double integrals, each double integral accounting for one internal coordinate. This is possible because the three internal coordinates are mutually independent of each other. The solution to each of the separated double integrals is exactly the same as the ones derived for the one-dimensional case. This simplification is another advantage of represent-

ing the population balance in terms of the volumes of solid, liquid and gas in the granules, rather than in terms of the total particle size, binder content and porosity.

4. Inverse problems in population balances

A generic issue in the development of population balance models is the identification of the model parameters employing appropriate experimental/plant data. However, in a number of situations, the underlying mesoscopic models are either unknown or are uncertain. In such cases, a grey-box strategy can be employed to directly identify the appropriate kernels from data. This leads to one form of the so-called Inverse Problem, and constitutes a crucial step in the use of population balances for many applications including granulation. It has found application for the identification of both aggregation kinetics as well as growth/nucleation kinetics.

Mahoney et al. (2002) developed a strategy for inverse problem solution to identify the growth and nucleation kinetics under aggregation/breakage-free conditions. Under nucleation and growth conditions, the solutions can be characterised employing the method of characteristics, with each solution emerging from either the initial condition or the boundary condition. This fact is exploited by the authors in identifying the growth and subsequently the nucleation kernels for such processes. They base their developments on the assumption that growth is deterministic and that the growth law is of the separable type, i.e., $G[l, t] = G_l(l) G_t[t]$. Thus, since $\mathrm{d}L/\mathrm{d}t = G[l, t]$, employing the above separable growth law, one obtains

$$
\int_{l_0}^{L(t|t_0, l_0)} \frac{\mathrm{d}l}{G_l(l)} = \int_{t_0}^{t} G_t[t]\, \mathrm{d}t,
\tag{4.1}
$$

where $L(t|t_0, l_0)$ denotes the size attained at time t along a particular characteristic that originates at (t_0, l_0). Further, along a given characteristic, the dilation/contraction of the distribution is governed by the following relationship:

$$
n(l, t) G_l(l) = n(l_0, t_0) G_l(l_0).
\tag{4.2}
$$

The size- and time-dependent portions of the growth law are represented in terms of chosen basis functions (such as the Hermite cubic basis functions) as follows:

$$
G_l(l) = \sum_{i=1}^{p} \alpha_i \phi_i(l) \quad \text{and}
$$

$$
G_t[t] = \sum_{i=1}^{z} b_i \psi_i(t).
\tag{4.3}
$$

The size-dependent portion can be combined with Eq. (4.2) to develop a system of equations that are regressed to data to identify the coefficients α_i. These are then used in Eq. (4.1) to determine the coefficients b_i in the time-dependent portion of the growth law.

Similar inverse problems for the determination of aggregation kinetics have been presented by Wright and Ramkrishna (1992). In the latter study, the method of weighted residuals is employed. Thus, as in their study on the extraction of the growth law, the aggregation kernel is expanded in terms of chosen basis functions and weighting polynomials, with the coefficients of expansion being determined by regressing with data. They demonstrate the extraction of the aggregation kernels both with and without continuous growth terms.

The aggregation kernel is sought of the form: $a(l, l', y) = \sum_j \alpha_j \phi_j(l, l', y)$. The residual to the population balance equation for any chosen weighting function $\psi_i(l, t)$ is given by

$$r_i = \int_{l=0}^{\infty} dl \int_{t=0}^{\infty} dt \, \psi_i(l, t)$$

$$\times \left[\frac{\partial n}{\partial t} + \frac{\partial}{\partial l} (G(l, y) n(l, t)) \right] - \sum_j A_{i,j} \alpha_j$$

$$A_{i,j} = \frac{1}{2} \int_{l=0}^{\infty} dl \int_{t=0}^{\infty} dt \int_{l'=0}^{l} \psi_i(l, t) \phi_j(l', \sqrt[3]{l^3 - l'^3}, y)$$

$$\times n(l', t) n(\sqrt[3]{l^3 - l'^3}, t)$$

$$\times \frac{l^2 dl'}{(l^3 - l'^3)^{2/3}} - \int_{l=0}^{\infty} dl \int_{t=0}^{\infty} dt \int_{l'=0}^{\infty}$$

$$\times \psi_i(l, t) \phi_j(l, l', y) n(l, t) n(l', t) dl'. \tag{4.4}$$

The formulation accounts for the (in)-frequency of measurements by employing a linear interpolation for the particle density between two measurements. Different weights α_j are identified for each time interval between measurements. Thus, for the aggregation-only case, the residual for the time interval k is given by the following equation:

$$r_{i,k} = \int_{l=0}^{\infty} \psi_i(l, t) [n(l, t_{k+1}) - n(l, t_k)] \, dl - \sum_j A_{i,j} \alpha_j,$$

$$A_{i,j,k} = \frac{1}{2} \int_{l=0}^{\infty} dl \int_{t=t_k}^{t_{k+1}} dt \int_{l'=0}^{l} \psi_i(l, t)$$

$$\times \phi_j(l', \sqrt[3]{l^3 - l'^3}, y) n(l', t) n(\sqrt[3]{l^3 - l'^3}, t)$$

$$\times \frac{l^2 dl'}{(l^3 - l'^3)^{2/3}} - \int_{l=0}^{\infty} dl \int_{t=t_k}^{t_{k+1}} dt \int_{l'=0}^{\infty}$$

$$\times \psi_i(l, t) \phi_j(l, l', y) n(l, t) n(l', t) \, dl'. \tag{4.5}$$

The PSD data are used to regress the coefficient so as to minimise the residuals.

For aggregation in combination with growth, the growth effects are added to the above formulation by moving the weighting function $\psi_i(l, t)$ along its characteristic growth curve. Thus, $\psi_i(l, t) = \psi_i(l_0(l, t))$, where $l_0(l, t)$ is derived implicitly from the growth law $dl/dt = G(l, t)$.

5. Application of modelling techniques for control and optimization

Many continuous granulation plants operate well below the design capacity, suffering from high recycle rates, and even instabilities induced by disturbance amplification effects (Zhang et al., 2000; Wang and Cameron, 2002). Thus, there is an immediate economic incentive for better understanding and for effective operation and control of granulation units. In batch operation, it is of interest to develop a systematic strategy for scale-up of high-value added products. Further, advanced control objectives for granulation operation include the granule particle size distribution, which finds correlation with several end-use properties covering various process industries including delivery rates of drugs/fertilisers/detergents, taste of food products, etc. The process is highly integrated and interacting, comprising drying units, classification, grinding units and recirculation loops, with limited manipulated variables available for operation and advanced control. Each of these factors motivate a fundamental model-based strategy for effective understanding, design, operation and control of granulation processes, employing either the population balance models described in Section 3 or other control-relevant models.

5.1. Sensitivity and controllability analysis

A desirable prerequisite for control is the analysis of the controllability of the process—the identification of suitable manipulated variables, the availability of sensors for critical product attributes, and the quantification of the limitations in these two fronts and their effect on the desired control. Thus, it is of relevance to discuss these issues before dealing with the application of control in granulation processes even though part of these may not fall under the systems perspective of research in granulation. Although there is scope for much advancement through further research in these areas, the studies reported up to this time serve as excellent reference for control development.

Mort et al. (2001) highlight the challenges in the control of granulation processes. They identify the importance of the control of granule density and the particle size distribution. They point out that sensors for critical product attributes such as the bulk density and PSD are available with large measurement delays. They also highlight the scarcity in terms of the manipulated variables—namely, the binder spray, mixing/tumbling rate. Thus, they identify a strategy based on a combined feedback and feedforward control for PSD, and a predominantly feedforward open-loop control for the bulk density. The latter is dictated by the large time delay associated with the measurement of the bulk density, the sensors for the same being located downstream of the drier, the time constant of which is comparable or greater than that of the granulator itself.

On a related note, Bardin et al. (2004) discusses the possibilities of enhancing the manipulated handles on the process through using multi-impeller mixer blades. They also advocate the use of the torque of the mixer or the work done in the agitation as an indicator of the particle size, to enable faster measurement of this quantity.

5.2. Modelling for closed-loop control purposes

5.2.1. Development of control relevant, linear models

Since linear control theory and techniques are better developed and easier to implement than their non-linear counter-parts, it is highly desirable to use linear models for control purposes. In process engineering, the non-linear models are frequently linearized around certain operating points. The general non-linear system is described as

$$\frac{d\mathbf{x}}{dt} = \mathbf{f}(\mathbf{x}, \mathbf{u}),$$
$$\mathbf{y} = \mathbf{h}(\mathbf{x}), \tag{5.1}$$

where $\mathbf{x} = [x_1\ x_2\ \ldots\ x_p]^T$, $\mathbf{y} = [y_1\ y_2\ \ldots\ y_q]^T$, and $\mathbf{u} = [u_1\ u_2\ \ldots\ u_s]^T$ are vectors of state, output and control variables, respectively. Also, $\mathbf{f} = [f_1\ f_2\ \ldots\ f_p]^T$ and $\mathbf{h} = [h_1\ h_2\ \ldots\ h_q]^T$ are vectors of smooth functions, in which p, q, and s are dimensions of the vectors of state, output and control variables, respectively. In the population balance equations given by Eqs. (3.3) and (3.4), $x = [n_1\ n_2\ \ldots\ n_p]$, $p = i_{max}$. In the conventional method, linearization is based on the first order Taylor series expansion around certain operational points. The resulting linear model is given by

$$\frac{d\delta\mathbf{x}}{dt} = \mathbf{A}\delta\mathbf{x} + \mathbf{B}\delta\mathbf{u},$$

$$\delta\mathbf{y} = \mathbf{C}\delta\mathbf{x},$$

$$\mathbf{A} = \left.\frac{\partial\mathbf{f}(\mathbf{x}, \mathbf{u})}{\partial\mathbf{x}^T}\right|_{\substack{x=x_o \\ u=u_o}},$$

$$\mathbf{B} = \left.\frac{\partial\mathbf{f}(\mathbf{x}, \mathbf{u})}{\partial\mathbf{u}^T}\right|_{\substack{x=x_o \\ u=u_o}},$$

$$\mathbf{C} = \left.\frac{\partial\mathbf{h}(\mathbf{x})}{\partial\mathbf{x}^T}\right|_{\substack{x=x_o \\ u=u_o}}. \tag{5.2}$$

In the control literature, the symbol δ in front of x, y and u is normally omitted for simplicity. Models developed this way mean that x, y and u denote deviations from their respective values at the specified operational point rather than the real values. That is, the linearized model used in control studies is represented as

$$\frac{d\mathbf{x}}{dt} = \mathbf{A}\mathbf{x} + \mathbf{B}\mathbf{u},$$
$$\mathbf{y} = \mathbf{C}\mathbf{x}. \tag{5.3}$$

The discretised population balance equations given by Eqs. (3.3) and the binder size distribution model described by Eq. (3.4) can be linearized to obtain the models with the format given by Eq. (5.3). The control variables are normally connected with the coalescence kernels (Zhang et al., 2000).

5.2.2. ARX and ARMAX models for linear model predictive control

For model predictive control purposes, there are two commonly used black-box models: ARX model with autoregressive (AR) part and extra (X) input, and ARMAX model with additional moving average (MA) part accounting for disturbances. The method for the development of ARX and ARMAX models is well explained in the book by Ljung (1987). The single input, single output ARX is given by

$$y(t) + a_1 y(t-1) + \cdots + a_{n_a} y(t - n_a)$$
$$= b_1 u(t-1) + \cdots + b_{n_b} u(t - n_b) + e(t) \tag{5.4}$$

and the ARMAX model is represented as

$$y(t) + a_1 y(t-1) + \cdots + a_{n_a} y(t - n_a)$$
$$= b_1 u(t-1) + \cdots + b_{n_b} u(t - n_b) + e(t) + c_1 e(t-1)$$
$$+ \cdots + c_{n_c} e(t - n_c). \tag{5.5}$$

In Eqs. (5.4) and (5.5), y is the output (controlled) variable, u is the input (manipulative) variable, e is the disturbance, a, b and c are time varying coefficients identified on-line, n_a, n_b and n_c are defined as prediction, control and disturbance horizons. The matrix format for multivariable ARX and ARMAX models are described by

$$\mathbf{A}(q)\mathbf{y}(t) = \mathbf{B}(q)\mathbf{u}(t) + \mathbf{e}(t) \quad (ARX), \tag{5.6}$$

$$\mathbf{A}(q)\mathbf{y}(t) = \mathbf{B}(q)\mathbf{u}(t) + \mathbf{C}(q)\mathbf{e}(t) \quad (ARMAX). \tag{5.7}$$

In Eqs. (5.6) and (5.7), matrices $\mathbf{A}$, $\mathbf{B}$ and $\mathbf{C}$ are defined as

$$\mathbf{A}(q) = \mathbf{I}_{n_y} + \mathbf{A}_1 q^{-1} + \cdots + \mathbf{A}_{n_a} q^{-n_a},$$
$$\mathbf{B}(q) = \mathbf{B}_1 q^{-1} + \cdots + \mathbf{B}_{n_b} q^{-n_b},$$
$$\mathbf{C}(q) = \mathbf{I}_{n_y} + \mathbf{C}_1 q^{-1} + \cdots + \mathbf{C}_{n_c} q^{-n_c}, \tag{5.8}$$

where q^{-k} is the delay operator representing "delayed by k time intervals", for example:

$$\mathbf{A}(q)\mathbf{y}(t) = \mathbf{y}(t) + \mathbf{A}_1 \mathbf{y}(t-1) + \cdots + \mathbf{A}_{n_a}\mathbf{y}(t - n_a). \tag{5.9}$$

The compact format of ARX and ARMAX models given by Eqs. (5.6) and (5.7) can easily be converted into more intuitive, expanded format exemplified by Eq. (5.9). With input ($\mathbf{u}$ and $\mathbf{e}$) and output ($\mathbf{y}$) data, the matrices A, B and C can be readily identified employing the System Identification Toolbox for Use with MATLAB^{TM} (Ljung, 2000). An ARX model for a pan granulation process was developed by Adetayo et al. (1997) with a successful application to effective control of the plant.

5.2.3. Model predictive control

Model predictive control (MPC) schemes consist of simultaneous determinations of manipulative variables and uncertain parameters. In some cases, the open-loop dynamic
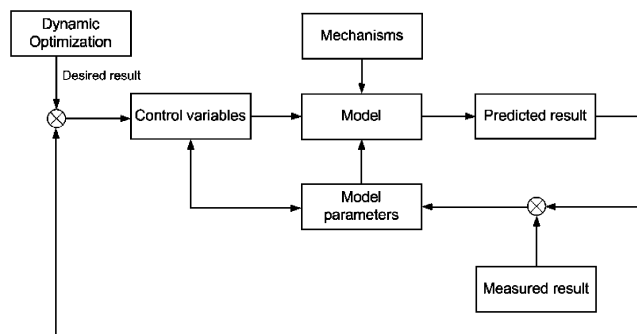
Fig. 6. General structure of NMPC using physically based models.

optimisation is carried out for the determination of desired trajectories (set-points). This integrated control strategy was developed by Miller and Rawlings (1994) in a study on model identification and control for batch cooling crystallisers, in which the population balance described by partial differential equations was reduced to a low dimensional model using the method of moments. That is, the control objective was average size rather than size distribution in Miller and Rawlings' work. Detailed studies on modelling and model predictive control (MPC) of particle size distribution in emulsion co-polymerisation processes using population balance models have been carried out by Immanuel and Doyle III (2003b) and Crowley et al. (2000). The reported research results have shown that the NMPC schemes using population balance equations should also be applicable to granulation processes due to the similar model structure. A general structure for non-linear model predictive control is shown in Fig. 6, which depicts an integration of the modelling strategy originally proposed by Sanders et al. (2003) with the model based control scheme.

A simulated study has been carried out by Zhang et al. (2000) to control an industrial scale fertiliser plant using a physically based model. The main limitation of the study was that the physically based population balance model was used to generate output data without real on-line measurements. This implies that if a severe plant-model mismatch occurs, the proposed control strategy may fail. Further work is required to modify the model on-line, based on the measurement data.

Pottmann et al. (2000) demonstrated the control of granule density and the granule size in continuous operation of industrial granulators. They proposed a model predictive control strategy in which the control of the granule size is achieved through the control of the 5th percentile and the 90th percentile of the particle sizes. In their granulation system, they employ three binder addition ports as the manipulated variables, each of which influence the bulk density, and the 5th and the 90th percentiles of the particle sizes. They point out that independent control of both the 5th and the 90th percentile is not possible. Thus, to avoid infeasibility, they seek to set one-sided constraints for these two variables (rather than require set-point tracking). They employ

a linear MPC framework based on a discrete time first-order plus time delay transfer function model.

The control problem is defined as follows:

$$\rho_B(k) = \rho_B^r(k),$$
$$d_5(k) \geqslant d_L,$$
$$d_{90}(k) \leqslant d_U, \tag{5.10}$$

subject to : $n_i^{\min} \leqslant n_i(k) \leqslant n_i^{\max}$ for $i = 1, 2, 3.$

In the above formulation, $\rho_B(k)$ is the bulk density at the discrete time instant k and $\rho_B^r(k)$ is the set-point value at the same time instant. $n_i(k)$ is the binder addition rate at time instant k through nozzle i. The optimisation problem underlying the MPC strategy is given below:

$$\min_{U(k)} I = \sum_{i=1}^{P} e^{\mathrm{T}}(k+i) W e(k+i) + \sum_{i=0}^{C-1} u^{\mathrm{T}}(k+i) Q u(k+i), \tag{5.11}$$

where $e(k+i)$ is the vector of error in the output at time instant $k+i$, and $u(k+i)$ is the input at the same time instant. The objective seeks to minimise the deviation of the output from the desired value with the minimal variation of the inputs from their nominal values. They simplify the above optimisation problem by separating the effects of the past control actions on the evolution of the outputs from those of the future control actions (the future control actions being the decision variables for the optimization problem). This results in the formulation shown below:

$$\min_{U(k)} I = U^{\mathrm{T}}(k)[M^{\mathrm{T}} \bar{W} M + \bar{Q}] U(k) - 2X^{\mathrm{T}}(k) \bar{W} M U(k) + X^{\mathrm{T}}(k) \bar{W} X(k), \tag{5.12}$$

$$X(k) = Y^r(k) - \hat{Y}^p(k) - \psi(k),$$
$$E(k) = X(k) - M U(k).$$

The matrix M is related to the process model. The constraints on the inputs and the outputs (bounds on the particle size) are set as follows:

$$\begin{bmatrix} I \\ -I \end{bmatrix} U(k) \leqslant \begin{bmatrix} \underbrace{u_{\max}^{\mathrm{T}} \cdots u_{\max}^{\mathrm{t}}}_{C\text{times}} - \underbrace{u_{\min}^{\mathrm{T}} \cdots -u_{\min}^{\mathrm{t}}}_{C\text{times}} \end{bmatrix}^{\mathrm{T}}, \tag{5.13}$$

$$\begin{bmatrix} M \\ -M \end{bmatrix} U(k) \leqslant \begin{bmatrix} Y_{\max} + X(k) - Y^r(k) \\ -Y_{\min} - X(k) + Y^r(k) \end{bmatrix}. \tag{5.14}$$

In their study, they identified the need for the prioritisation of the objectives, as well as the need for relaxing hard constraints at the initial steps of the prediction horizon to avoid infeasibility of the optimisation problem.

Gatzke and Doyle III (2001) propose a model predictive controller based on two novel strategies to both account for the prioritisation and to avoid the infeasibilities in the optimization problems. One of these is based on a soft constraint

control. The other is based on a prioritised control strategy so as to avoid unattainable set-points as well as to tackle the more important objectives first and the less important ones later. Along the lines of Pottmann et al. (2000) they develop controls for the bulk density along with the 5th and 90th percentiles of the particle size. Also, as in Pottmann et al., they required reference (set-point) tracking for bulk density, while the 5th and the 90th percentiles of the particle sizes were constrained between set limits. In order to address infeasibility concerns in optimization problems, Gatzke and Doyle III (2001) proposed two alternative model predictive control strategies. The first strategy is a direct extension of traditional MPC, with either a quadratic or a linear objective function, and constraints (either one- or two-sided) for the objectives on particle size.

$$\min \quad \tfrac{1}{2} x_x^T H x_c + c^T x_c$$
$$\text{s.t.} \quad a x_c^T \leqslant b; \quad \underline{x} \leqslant x_c \leqslant \overline{x}. \tag{5.15}$$

Soft constraints on the outputs:

$$r(i) - \hat{y}(i) \leqslant e_y(i) \quad \text{and} \quad -r(i) + \hat{y}(i) \leqslant e_y(i)$$
$$\forall i = k, k+1, \dots, k+p. \tag{5.16}$$

In the above equation, $r(i)$ is the reference or set-point value at discrete time instant i, $y(i)$ is the measurement at time instant i, k is the current time instant, and p denoted the prediction horizon (the number of time instants into the future over which the error is sought to be minimised).

For the objectives on the 5th and 90th percentiles on the particle size, they have envisaged the need for asymmetric constraints, for which they propose the following asymmetric bounds:

$$r_o(i) - \hat{y}_o(i) \leqslant \alpha_0^+ e_{yo}(i) \quad \text{and}$$
$$-r_o(i) + \hat{y}_o(i) \leqslant \alpha_0^- e_{yo}(i)$$
$$\forall i = k, k+1, \dots, k+p. \tag{5.17}$$

In the above equation, the subscript o refers to a particular control objective. A suitable choice of the values of α_0^+ and α_0^- will ensure the realization of the necessary asymmetric bounds on the control objectives.

The second control strategy is based on a prioritised objective formulation. This is inspired by the need for prioritising the objectives (economical versus product properties) or to enable a step-by-step facilitated approach to the set-point value. In this strategy, they specify a series of control objectives and assign priorities for each of them. The objective function in the formulation is given by

$$\min_{u, o, p} \quad -P_1 p - P_2 o + \sum_{i=k}^{k+p} \| \Gamma_y(r(i) - \hat{y}_p(i)) \|_1$$
$$+ \sum_{i=k}^{k+m} \| \Gamma_u \Delta u(i) \|_1, \tag{5.18}$$

$$p_j, o_j \in \{0, 1\}.$$

In this equation, the last two terms represent the traditional output error and move suppression terms. The first two terms are added to prioritise the outputs. The binary variables o_j assume a value of 1 if the control objective j is satisfied (for any given solution u). If any particular control objective i is not satisfied, then the corresponding priority p_i is set to a value of 0 (in addition to o_i being 0). Further, the priority variables p_j for all other control objectives of a lower priority than the said control objective i are also set to 0. These logics are represented by the following constraints:

$$p_1 \leqslant o_1; \ p_2 \leqslant o_2; \ \dots p_N \leqslant o_N,$$
$$p_2 \leqslant p_1; \ p_3 \leqslant p_2; \ \dots p_{N-1} \leqslant p_N. \tag{5.19}$$

In these constraints, the subscripts refer to the N control objectives of decreasing priority.

The weight P_1 is assigned a larger value than the weight P_2, and both of these are maintained higher than typical values of the output error and move-suppression terms (through suitable choice of weights Γ_y and Γ_u). Thus, the solution u seeks to maintain the ordered priorities of the control objectives foremost, then ensures as many control objectives are satisfied as possible, and finally addresses the errors in the reference tracking and the move suppression terms.

Wildeboer (2002), in his Ph.D. dissertation at the University of Queensland, has developed an effective strategy for operation and control of granulators based on regime separation. In this strategy, he proposes the separation of the various processes that determine the granule properties, namely wetting and nucleation, aggregation and growth, breakage and attrition, into separate vessels. It is clear that this approach provides better handle and enhances the attainable region. A similar strategy was successfully applied for emulsion polymerisation problems (Immanuel and Doyle III, 2003b), resulting in a facilitated approach for the underlying complex non-convex optimisation problem. Thus, this regime-separation strategy is promising for future nonlinear control developments.

5.2.4. On-line measurement-based control schemes

In addition to model-based control schemes using population balance equations, there are a number of practical control schemes in the pharmaceutical industry, which do not rely on mathematical models. These include simple feedback control with or without feed-forward compensation, and fuzzy-logic control systems.

5.2.4.1. Simple feedback control with feed-forward compensation One of the most important issues for the effective control of granulation processes is the development of fast and reliable measurement techniques for the characterisation of particulate systems. Because of the difficulties associated with the direct measurement of particle characteristics, such as particle size distribution, moisture contents and deformability, some indirect monitoring parameters have been adopted as the indicators of particle characteristics. A commonly accepted monitoring parameter in the pharmaceutical
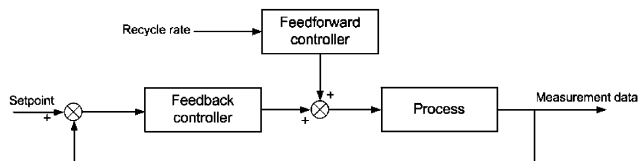
Fig. 7. Simple feedback control scheme with feed-forward compensation.

Fig. 8. Block diagram of granule size control system (after Watano et al., 2001a).

industry is the power consumption, which has been success-fully used to control the particle size in high-shear mixers at the end-point (Leuenberger, 1994; Faure et al., 2001). Based on a series of investigations carried out by Leuenberger (1994), the energy dissipated per unit volume in a high-shear mixer, dW/dV, can be approximately represented as

$$\frac{dW}{dV} = \mu \sigma_c \kappa \propto \frac{1-\varepsilon}{\varepsilon}, \tag{5.20}$$

where W is the power consumption, V is the granulator volume, μ is the apparent coefficient of friction, σ_c is the cohesive stress, κ is the dimensionless shear rate, and ε is the porosity of the powder mass. It is easy to show that the power consumption is related to the saturation level S defined as follows:

$$S = \frac{H(1-\varepsilon)}{\varepsilon}\rho, \tag{5.21}$$

where H is the mass ratio of liquids to solids, and ρ is the density of the particle relative to the density of the liquid ($\rho = \rho_S/\rho_L$). Furthermore, Kristensen and Schaefer (1987) pointed out that the saturation level defined by Eq. (5.21) could be related back to the average granule size. Consequently, the power consumption, the saturation level and the granule particle size are inter-related, which forms a technical basis to use power consumption as a monitoring parameter for the characterisation of particles within the high-shear mixer. A detailed description of the control strategy using power consumption as the indicator of particle properties in high-shear mixers is also provided in Leuenberger (1994).

Mort and co-workers pointed out that: "With recent development in particle sizing technology, the agglomerate size distribution can be measured in-line at any number of points in the process." (Mort et al., 2001). The main measurement technique is image-analysis by mounting high-speed cameras and lighting systems in appropriate locations. Since the direct measurement data of particle sizes are available, the controller design can be based on these data without relying on the indirect indicators under the condition that the rate of binder addition is sufficiently slow to allow for image data to be collected, processed and fed back. This concept has been used for batch granulation processes in fluidised beds. The same authors (Mort et al., 2001) also proposed a feed-forward control strategy to compensate the fluctuation of the recycle rate. The simple feedback control with feed-forward compensation scheme is shown in Fig. 7.

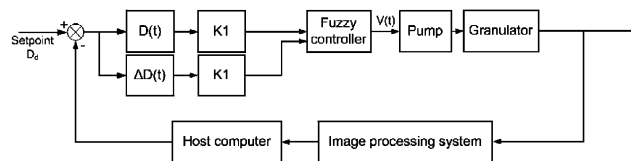The measurement data in Fig. 7 could be the indirect monitoring parameters (Leuenberger, 1994), or the explicit

particle size distribution (Mort et al., 2001), depending on the relative speed of the measurement system and process dynamics.

A few relevant sensors for the monitoring and on-line control of granulation processes include; focussed beam reflectance measurement and Particle vision measurement for on-line PSD measurement (Lasentec), acoustic probe (Wildeboer, 2002).

5.2.4.2. Fuzzy-logic control of high-shear granulation
Watano et al. (2001a,b) have developed a novel system to control granule growth in a high-shear mixer. The system basically consisted of image processing and a fuzzy controller as shown in Fig. 8.

In Fig. 8, $D(t)$ is the deviation between the desired value (D_d) and measured value (D_m) of granule size, and $\Delta D(t)$ denotes the change rate of measured values, which are mathematically represented as follows:

$$D(t) = D_d - D_m(t),$$
$$\Delta D(t) = D_m(t) - D_m(t-1), \tag{5.22}$$

$V(t)$ is the result of fuzzy reasoning used to control the output power of liquid feed pump, K_1 and K_2 represent gains of the input variables.

In the methodology developed by Watano et al. (2001a,b), four fuzzy variables were used, namely ZR (zero), PS (positive small), PM (positive medium) and PL (positive large). The values of $D(t)$, $\Delta D(t)$ and $V(t)$ were all classified into these four categories. Ten rules were proposed to relate measured $D(t)$ and $\Delta D(t)$ with $V(t)$. Consequently, $V(t)$ can be quantified using the if-then statement. An example is given as follows:

If $D(t) = $ PS and $\Delta D(t) = $ PL then $V(t) = $ ZR (Rule 2 in Table 2 of Watano et al. (2001b)).

In such a way, all the combinations of $D(t)$ and $\Delta D(t)$ can be connected with $V(t)$ for the effective control of the process.

5.3. Modelling for optimal design, operation and open-loop optimal control

Process optimisation and open-loop optimal control of batch and continuous drum granulation processes are another important application example of population balance modelling. Both steady state and dynamic optimisation studies consist of: (i) construction of optimisation and control
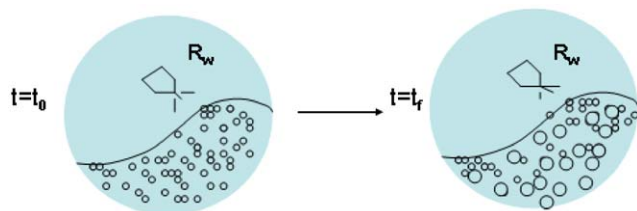
Fig. 9. Schematic diagram of batch drum granulation.

Fig. 10. Schematic diagram of continuous drum granulation.

relevant, population balance models through the incorporation of moisture content, drum rotation rate and bed depth into the coalescence kernels; (ii) investigation of optimal operational conditions using constrained optimisation techniques; and (iii) development of optimal control algorithms based on discretised population balance equations. The objective of steady state optimisation is to minimise the recycle rate with minimum cost for continuous processes. It has been identified that the drum rotation-rate, bed depth (material charge), and moisture content of solids are practical decision (design) parameters for system optimisation. The objective for the optimal control of batch granulation processes is to maximise the mass of product-sized particles with minimum time and binder consumption. The objective for the optimal control of the continuous process is to drive the process from one steady state to another in a minimum time with minimum binder consumption, which is also known as the state-driving problem. It has been known for some time that the binder spray-rate is the most effective control (manipulative) variable. Although other process variables, such as feed flow-rate and additional powder flow-rate can also be used as manipulative variables, only the single input problem with the binder spray rate as the manipulative variable is addressed here to demonstrate the methodology. It can be shown from simulation results that the proposed models are suitable for control and optimisation studies, and the optimisation algorithms connected with either steady state or dynamic models are successful for the determination of optimal operational conditions and dynamic trajectories.

5.3.1. Statement of optimisation and open-loop optimal control problems

A typical batch drum granulation process is schematically shown in Fig. 9. There are two operational strategies: (1) pre-mix the fine particles with the proper amount of liquid binder followed by the rotating operation until the desired size distribution is achieved; and (2) simultaneous mixing and granulating by spraying liquid binder (and fine powders in some cases) on the moving surface of particles inside the rotating drum. The first strategy involves system optimisation without any control action. The optimisation problem can be stated as: to determine the optimal moisture content, initial size distribution, rotating rate and bed depth (drum charge), such that the desired size distribution can be obtained within a minimum time t_f. Optimal control
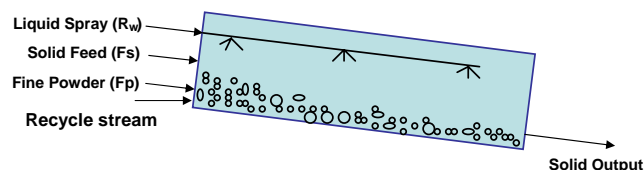
techniques can be applied to the second strategy, which can be stated as: for the specified initial conditions, maximize the mass of product-sized particles in minimum time with minimum energy consumption by adjusting the manipulative variables, such as binder spray-rate and drum rotation speed.

A slightly modified continuous drum granulation process with an additional fine powder stream is shown in Fig. 10. As mentioned previously, the additional fine powder stream is used to improve the controllability of the process, which is not seen in the conventional design. Studies on continuous drum granulation include the steady state optimisation and optimal state driving from one steady state to another. The objective for steady state optimisation is to achieve minimum recycle rate with minimum cost through the determination of optimal operational conditions, such as rotating rate, binder spray rate, feed flow-rate, bed-depth, and drum inclination angle. Optimal state driving attempts to drive the system from one steady state to another in a minimum time with minimum energy consumption by adjusting the time dependent manipulative variables, such as binder spray rate, feed flow-rate and optionally additional fine powder flow-rate.

5.3.2. Optimisation and open-loop optimal control description

The optimisation and open-loop control descriptions consist of model equations and objective functions.

5.3.2.1. Optimisation and control relevant model equations
The discretised population balance equation for batch system can be described as follows:

$$\frac{\mathrm{d}}{\mathrm{d}t} n_i = -\frac{\partial}{\partial L}(Gn_i) + B_i - D_i,$$
$$i = 1, 2, \ldots, i_{\max}, \tag{5.23}$$

where n_i, B_i and D_i stand for the particle number, birth rate and death rate in the ith size interval, respectively, $i = 1, 2, \ldots, i_{\max}$, in which $i_{\max}$ is the total number of size intervals. Similarly, continuous processes can also be represented as

$$\frac{\mathrm{d}}{\mathrm{d}t} n_i = -\frac{\partial}{\partial L}(Gn_i) + B_i - D_i$$
$$+ F^{\mathrm{in}} \frac{n_i^{\mathrm{in}}}{n_t^{\mathrm{in}}} - F^{\mathrm{out}} \frac{n_i}{n_t},$$
$$i = 1, 2, \ldots, i_{\max}, \tag{5.24}$$

where F is the number flow-rate, the subscript t indicates the total value, and the superscripts identify the inlet and outlet streams. Using Hounslow's discretisation methods, the relevant terms in the right hand sides of Eqs. (5.23) and (5.24) are given by

$$B_i = n_{i-1} \sum_{j=1}^{i-2} (2^{j-i+1} \beta_{i-1,j} n_j) + \frac{i}{2} \beta_{i-1,i-1} n_{i-1}^2, \quad (5.25)$$

$$D_i = n_i \sum_{j=1}^{i-1} (2^{j-i} \beta_{i,j} n_j) - n_i \sum_{j=1}^{i_{max}} (\beta_{i,j} n_j), \quad (5.26)$$

$$\frac{\partial G n_i}{\partial L} = -\frac{2G}{(1+r)L_i} \\ \times \left(\frac{r}{r^2-1} n_{i-1} + n_i - \frac{r}{r^2-1} n_{i+1} \right), \quad (5.27)$$

$$r = L_{i+1}/L_i = \sqrt[3]{2},$$

where $\beta_{i,j}$ is equivalent to the representation $\beta(L_i, L_j)$. Consequently, an original population balance equation described by a partial differential-integral equation is converted into a set of ordinary differential equations.

A control relevant model was developed by Zhang et al. (2000), in which the coalescence kernel is a function of the moisture content. In the newly developed kernel models reported by Wang et al. (2004, 2005), in addition to moisture content, the bed depth and drum speed are also incorporated. Two kernel models, namely size independent kernel and size dependent kernel, are used in optimisation and control simulations. The size independent kernel is given by

$$\beta_{i,j} = \beta_0 = a_0 \cdot [(x_m)^{n_1} e^{-a_1 x_m}] \\ \cdot [(B_d)^{n_2} e^{-a_2 B_d}] \cdot (S_d^{n_3} e^{-a_3 S_d}), \quad (5.28)$$

where x_m is the moisture content in particles, B_d is the bed depth, S_d is the drum rotating rate, $a_0 - a_3$ and $n_1 - n_3$ are constants determined through parameter identification techniques based on the measurement data. The size dependent kernel is represented as (Friedlander, 2000):

$$\beta_{i,j} = \beta_0 \frac{(L_i + L_j)^2}{L_i L_j}, \quad (5.29)$$

where β_0 is also defined in Eq. (5.28).

Since the main mechanism determining the growth rate G in Eqs. (5.23) and (5.24) is layering of the fine powders on the surface of particles, it can be deduced that the growth rate is a strong function of the powder fraction and moisture content. The following correlation is used to calculate the growth rate:

$$G = G_m \cdot \frac{M_{powder}}{k \cdot \sum M_i + M_{powder}} \\ \cdot \exp[-a(x_w - x_{wc})^2], \quad (5.30)$$

where G_m is the maximum growth rate, M_{powder} is the mass of fine powder below the lower bound of the particle classes,

M_i is the mass of particles in the ith size class, x_{wc} is the critical moisture, k and a are fitting parameters. Studies on powder mass balance lead to the following equation for batch processes:

$$\frac{dM_{powder}}{dt} = F_{powder}^{in} - 3G \int_0^\infty \frac{M(L)}{L} dL, \quad (5.31)$$

and the following equation for continuous processes:

$$\frac{dM_{powder}}{dt} = F_{powder}^{in} - \frac{M_{powder}}{t_R} - 3G \int_0^\infty \frac{M(L)}{L} dL, \quad (5.32)$$

where F_{powder}^{in} represents the flow-rate of additional powder stream in both batch and continuous cases. It can be used as an additional manipulative variable.

The liquid mass balance for batch processes is given by

$$\frac{dx_w}{dt} = \frac{1}{M_t} R_w, \quad (5.33)$$

where M_t is the total mass of solids in the drum, R_w is the binder spray rate. Similarly, we can develop the liquid mass balance for the continuous process as

$$\frac{dx_w}{dt} = \frac{1}{M_t} [F_M^{in} x_w^{in} - F_M x_w + R_w], \quad (5.34)$$

where F_M^{in} and F_M are inlet and outlet mass flow-rates, respectively, and x_w^{in} is the moisture content in the feed solids.

In summary, the equations in the control relevant model for batch systems are discretised population balance equations given by Eq. (5.23), powder dynamics described by Eq. (5.31), and liquid dynamics represented by Eq. (5.33). The corresponding equations for continuous processes are Eqs. (5.24), (5.32) and (5.34). Both cases share the same kernel models given by Eqs. (5.28) and (5.29), and growth-rate model described by Eq. (5.30).

5.3.2.2. Objective functions for system optimisation and open-loop optimal control The objective function for system optimisation of batch granulation is

$$\underset{S_d, B_d, x_w}{\text{Minimize}} \left\{ J = \frac{-w_1 M_p(t_f)}{t_f} \right\}$$
Subject to: Eq. (5.23). $\quad (5.35)$

The objective function for optimal control of batch granulation with the binder spray rate as the only manipulative variable is given by

$$\underset{R_w}{\text{Mimimize}} \left\{ \frac{-w_1 M_p(t_f) + w_2 \int_0^{t_f} R_w \, dt}{t_f} \right\}$$
Subject to: Eqs. (5.23), (5.31), and (5.33). $\quad (5.36)$

In Eqs. (5.35) and (5.36), M_p is the mass of product sized particles, w_1 and w_2 are weighting functions.

The objective function for steady state optimisation of continuous granulation is

$$\underset{S_d,B_d,F^{\text{in}},R_w}{\text{Minimize}} \; \{-w_1 F_p + w_2 R_w\}$$

Subject to:

Eqs. (5.24), (5.32), (5.34) with left hand sides

replaced by zero, $\quad$ (5.37)

where F_p is the mass flow rate of product sized particles.

For state driving, steady state optimisations are first performed for two different product specifications: the product range for steady state 1 (SS1) is 2–3.2 mm, whereas that for steady state 2 (SS2) is 3.2–5.0 mm, followed by driving the process from SS1 to SS2. The objective function for this optimal state-driving problem is described as

$$\underset{R_w}{\text{Minimize}} \left\{ J = \sum [w_{1,i}(N_i - N_i^{SS2})^2] \right.$$
$$\left. + w_2 \int_0^{t_f} R_w \, dt + w_3 t_f \right\}$$

Subject to:

Eqs. (5.24), (5.32), (5.34)

and zero derivatives at final time, $\quad$ (5.38)

where N_i^{SS2} denotes the number of particles in the ith size interval for steady state 2.

5.3.3. Dynamic optimization algorithm

It is not difficult to solve the steady state optimisation problems with algebraic constraints by using commercialised software packages and dynamic optimal control problems subject to differential-algebraic equations (DAE) using the algorithm proposed in this work. The basic structure of the dynamic optimisation algorithm employed is shown in Fig. 11.

In the dynamic optimisation algorithm depicted in Fig. 11, a control parameterisation technique (Teo et al., 1991) is used to discretise the originally continuous control variables. That is, a control (manipulative) variable $u(t)$ is represented by a set of piece-wise constant values, u_i, $i = 1, 2, \ldots, q$. These constants are treated as parameters to be determined by using dynamic optimisation algorithms.

5.3.4. Selected simulation results and discussion

Simulations for both batch and continuous granulation processes are based on a pilot plant drum granulator with the following parameters: length = 2 m, diameter = 0.3 m, nominal hold up = 40 kg, rotation rate = 25–40 rpm, retention time range = 6–10 min. The simulated optimal profiles for the batch processes are shown in Fig. 12 with two data sets with and without constraints on control action. The control constraints restrict lower and upper bounds on the control variables, as well as the gradient of the control actions. It can be seen from Fig. 12 that if the constraints on the control variable are inactive, very high spray rates at an early
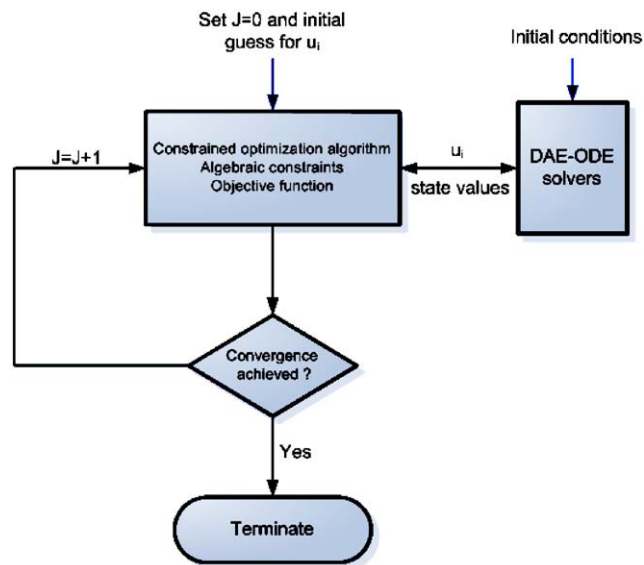

Fig. 11. Basic structure of the dynamic optimization algorithm.

operating stage with very short spray time leads to the minimum objective function given by Eq. (5.36). However, if these constraints are activated, the control variable moves smoothly rather than suddenly with the price of a longer operational time. The difference between final times in the two cases is about 104 s (283–179 s), which is quite significant.

Through steady-state optimisations, optimal binder spray rates for two different specifications on product size ranges are obtained. These are: $R_w = 0.050$ kg/s for 2.0–3.2 mm as the product size range, and $R_w = 0.075$ kg/s for 3.2–5.0 mm as the product size range. Fig. 13 shows the profiles using an optimal control policy and a constant spray rate policy. The optimal control policy leads to about 50% reduction on objective function given by Eq. (5.38). The optimal spray policy can be stated as: gradually increase the spray rate from the first steady state (0.005 kg/s) to achieve a relatively high spray rate (0.0084 kg/s) followed by gradual reduction of the spray rate until the spray rate of the second steady state value (0.0075 kg/s) is reached, which will be maintained for the rest of the operational period. From Fig. 13, the significance of optimal control studies can be demonstrated by observing the facts that the optimal profiles approach the second steady state faster, and the optimal control strategy is easy to implement with smooth movement.

Fig. 14 shows the dynamic profiles of optimal state driving from Steady State 1 to Steady State 2 with different levels of constraints. In addition to the constraints on control actions, the final time constraints to ensure the final steady state status are imposed on the system. That is, the left hand sides of Eqs. (5.24), (5.32) and (5.34) should be zero at the final time. However, it is not necessary to achieve zero exactly for the derivatives at the final time. We normally impose the final time constraints as $|dx(t_f)/dt| < \varepsilon$ in which x represents general state variables such as number of particles, mass of powder and moisture content, and ε is a very small positive
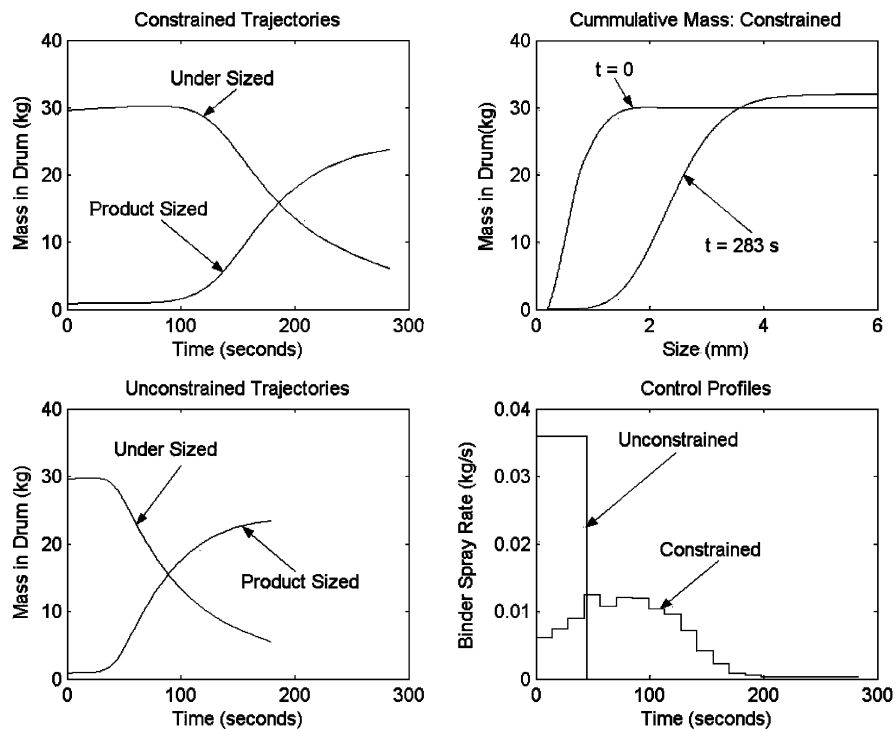
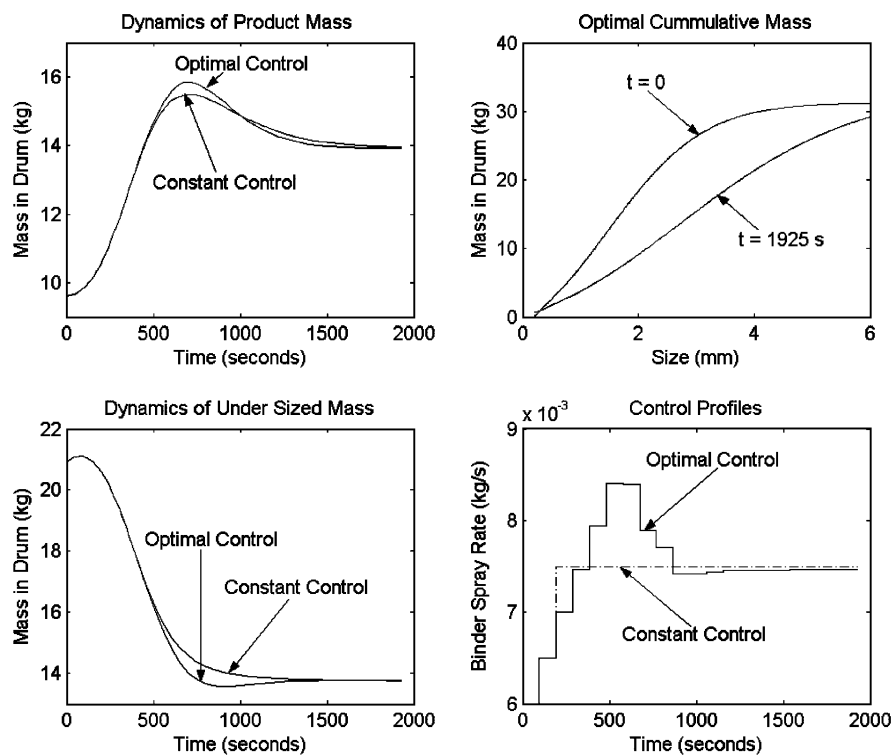Fig. 12. Optimal control of batch drum granulation.

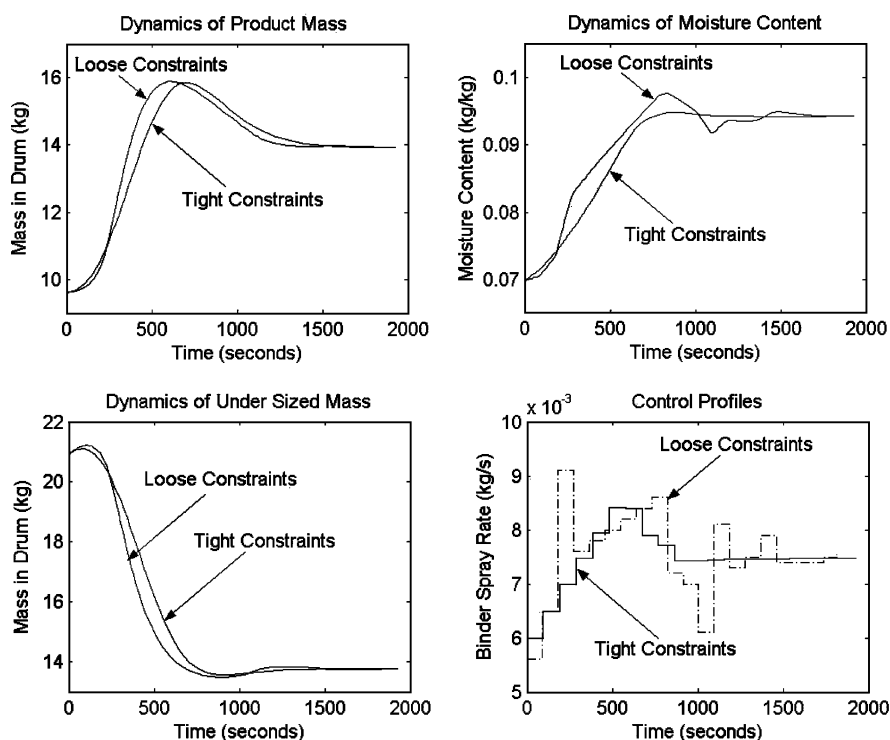Fig. 13. Optimal state driving of continuous drum granulation.

Fig. 14. Effect of constraint tightness on optimal control of drum granulation.

number for practical applications. The ε values are chosen as 10^{-6} and 10^{-3} for tight and loose constraints indicated in Fig. 14, respectively. It can be shown from Fig. 14 that the control strategy with loose constraints leads to shorter operational time than that with tight constraints (1827 vs. 1925 s). However, the moisture dynamics shows severe offset and oscillation. Furthermore, the control profile moves up and down, which is not easy to adjust. Since there is only 5% time reduction, the control strategy with tight constraints is superior to that with loose constraints in this particular application.

Through an analysis on the simulation results, the following conclusions can be drawn.

1. Population balance modelling is important to optimal design and operations for both batch and continuous granulation processes.
2. The effects of liquid content, bed-depth and drum rotation rate on the coalescence behaviour can be quantified through the development of new kernel models with the structure described by Eqs. (5.28) and (5.29). The simulation results are qualitatively consistent with industrial experience in large scale fertilizer production.
3. An optimal control strategy and algorithm using commercial optimisation software packages connected to reliable DAE/ODE solvers are successful for the determination of optimal trajectories with good convergence (Petzold, 1982; Cameron, 1983). This implies that under certain conditions, the more complicated optimal control

algorithms, such as that based on the well-known Pontryagin's maximum principle, could be avoided.
4. Since start-up and shutdown operations are frequently encountered in granulation plants with huge financial impacts, studies on optimal control strategies can lead to significant economic benefits.

5.4. On-line monitoring and diagnosis

Stable operation of granulation systems, especially continuous drum granulation has continued to be a major challenge. With the advent of detailed models of granulation circuits, it is now feasible to develop convincing monitoring and diagnostic systems.

As a basis of on-line monitoring and diagnoses, reliable on-line measurements of particle size distribution and moisture are important. The commonly used technique for on-line determination of particle size distribution in granulation is based on image analysis. A typical image analysis system consists of a CCD camera, lightning unit, telephoto lens and computer. An image probe is normally installed within the high shear granulator to receive the image, which has been described in detail by Watano et al. (2001a,b). A study of on-line size measurement based on image analysis using an OptiSizer unit (Webb and Orr, 1997) has been carried out at The University of Queensland for drum granulation processes (Wang and Cameron, 2002). The experimental set-up is shown at the URL: http://www.cheque.uq.edu.au/psdc. In contra st to the installation of a probe for the high shear

granulator, a sampling system can be developed for drum granulation processes to allow the measurement of a relatively small sample stream using the OptiSizer unit. In the case where the particles are wet, technical difficulties may occur due to the temporary agglomeration and reduced flowability induced by the particle stickiness. A modified strategy is to dry the particles before the measurement. However, this will lead to a further time delay.

Solid moisture can be measured on-line by using near-infrared (NIR) spectroscopy (Morris et al., 1998) or microwave-based techniques. A microwave technique for the measurement of solid moisture in batch samples has been developed by Shahhosseini et al. (1997). Its extension to continuous samples encounters similar difficulties to that of OptiSizer units due to the particle stickiness. Further work is needed to develop improved sensors for both particle size and moisture measurements.

Recent work by Schelbach (2000) developed a real-time expert system based on root-cause analysis derived from a comprehensive HAZOP study of the granulation circuit. It used deep knowledge on granulation derived from an understanding of the mechanisms that play a role in particle formation and breakage. The diagnostic system was implemented in G2 (Gensym, 2004) and tested using a detailed dynamic simulation of a commercial granulation circuit (Balliu et al., 2001).

In a further development, Nemeth et al. (2004 a,b) developed a hierarchical coloured Petri net (CPN) approach to the diagnosis problem by using a multiscale view that relied on a series of increasingly detailed models from circuit to equipment to mechanisms. This again relied on process models coupled with qualitative failure models that allowed the system to monitor operations and determine possible reasons for detected faults.

So far, it appears that there are no commercial real-time diagnosis applications. However, the current developments in academe have a high possibility of providing monitoring and model-based diagnosis in commercial operations.

6. Summary

Process systems modelling to address a range of issues in granulation is an area of growing importance. It is dominated by the population balance approach for developing models that incorporate both mechanistic and empirical elements, that is, grey-box methods. However, effective modelling requires an improved understanding of the key factors involved in particle growth and breakage. This is currently improving. As well, the growing importance of particulate flow patterns is being addressed through approaches such as discrete element methods (DEM) and CFD, that provide a micro-scale view of particle motions in the granulation device. The challenge is in addressing the multi-scale nature of granulation modelling that covers scales from the particle interactions up to and beyond the plant level.

The development of empirically based models has provided a simple means of addressing quickly a number of control related applications. This will continue to be a useful approach for such problems but cannot provide the long term benefits of a more phenomenological approach.

Application of models to design, advanced control and diagnosis will require mechanistic models that continue to incorporate the latest understanding of the underlying mechanisms. Much work is currently underway in these areas and the incorporation into existing models of new knowledge will help extend the applicability of process models for a wide range of granulation systems.

References

Abou-Chakra, H., Baxter, J., Tüzün, U., 2004. Three-dimensional particle shape descriptors for computer simulation of non-spherical particulate assemblies. Advanced Powder Technology 15, 63–77.

Adetayo, A.A., Ennis, B.J., 1997. A unifying approach to modelling granulation processes coalescence mechanisms. A.I.Ch.E. Journal 43 (1), 927–934.

Adetayo, A.A., Litster, J.D., Pratsinis, S.E., Ennis, B.J., 1995. Population balance modelling of drum granulation of materials with wide size distribution. Powder Technology 82, 37–49.

Adetayo, A.A., Pottman, M., Ogunnaike, B., 1997. Effective control of a continuous granulation process. Proceedings of the Control of Particulate Processes, vol. IV. Engineering Foundation, NY, pp. 23–28.

Akaike, H., 1970. Statistical predictor identification. Annals of Institute of Statistics and Mathematics 243–247.

Balliu, N., Cameron, I.T., Newell, R.B., 2001. Development of a Particle Processing Model Library for Process Design, Dynamics and Optimization. 6th World Congress on Chemical Engineering, Melbourne, Australia, September, Paper P3-138.

Bardin, M., Knight, P.C., Seville, J.P.K., 2004. On control of particle size distribution in granulation using high-shear mixers. Powder Technology 140, 169–175.

Biggs, C.A., Sanders, C., Scott, A.C., Willemse, A.W., Hoffman, A.C., Instone, T., Salman, A.D., Hounslow, M.J., 2003. Coupling granule properties and granulation rates in high-shear granulation. Powder Technology 130, 162–168.

Breipohl, A.M., 1970. Probabilistic Systems Analysis. Willey, New York.

Cameron, I.T., 1983. Solution of differential—algebraic systems using diagonally implicit Runge–Kutta methods. IMA Journal of Numerical Analysis 3, 273–289.

Cameron, I.T., Wang, F.Y., 2005. Granulation process modeling. In: Dilip Parikh (Ed.), Encyclopedia of Pharmaceutical Processing, second ed. Marcel-Dekker, New York, in press.

Charpentier, J.C., 2002. The triplet "molecular processes -product-process" engineering: the future of chemical engineering. Chemical Engineering Science 57, 4667–4690.

Crowley, T.J., Meadows, E.S., Kostoulas, A., Doyle III, F.J., 2000. Control of particle size distribution described by a population balance model of semi-batch emulsion polymerisation. Journal of Process Control 10, 419–432.

Cussler, E.L., Wei, J., 2003. Chemical product engineering. A.I.Ch.E. Journal 49, 1072–1075.

Ennis, B.J., Litster, J.D., 1997. Size enlargement. Perry's Chemical Engineering Handbook, seventh ed. McGraw-Hill, NY (Chapter 8).

Ennis, B.J., Tardos, G., Pfeffer, R., 1991. A microlevel-based characterization of granulation phenomena. Powder Technology 65, 257–272.

Faure, A., York, P., Rowe, R.C., 2001. Process control and scale-up of pharmaceutical wet granulation processes: a review. European Journal of Pharmaceutics and Biopharmaceutics 52, 269–277.

Friedlander, S.K., 2000. Smoke, Dust and Haze, first ed. Wiley, NY, 1977; second ed. Oxford University Press, NY.

Gantt, J.A., Gatzke, E.P., 2005. High shear granulation modeling using a discrete element simulation approach. Powder Technology, in press.

Gatzke, E.P., Doyle III, F.J., 2001. Model predictive control of a granulation system using soft output constraints and prioritized control objectives. Powder Technology 121, 149–158.

Goldschmidt, M.J.V., 2001. Hydrodynamic modelling of fluidised bed spray granulation. Ph.D. Thesis, University of Twente.

Gensym, 2004. http://www.gensym.com/

Goldschmidt, M.J.V., Weijersa, G.G.C., Boerefijn, R., Kuipers, J.A.M., 2003. Discrete element modelling of fluidised bed spray granulation. Powder Technology 138, 39–45.

Golovin, A.M., 1963. Soviet Physics Doklady 8, 191.

Gooch, J.R.P., Hounslow, M.J., 1996. MC simulation of size-enlargement mechanisms in crystallization. A.I.Ch.E. Journal 42 (7), 1864–1874.

Goodson, M.J., Kraft, M., Forrest, S., Bridgewater, J., 2004. A multi-dimensional population balance model for aggregation. In: Second International Conference on Population Balance Modelling.

Hangos, K.M., Cameron, I.T., 2001. Process Modelling and Model Analysis. Academic Press, London, ISBN 0-12-156931-4.

Heinrich, S., Peglow, M., Ihlow, M., Morl, L., 2003. Population balance modeling in fluidized bed-spray granulation—analysis of the steady state and unsteady behaviour. Powder Technology 130, 154–161.

Hogue, C., 1998. Shape representation and contact detection for discrete element simulations of arbitrary geometries. Engineering Computations 15, 374–390.

Hoomans, B.P.B., 1999. Granular dynamics of gas–solid two-phase flows. Ph.D. Thesis, University of Twente.

Hounslow, M.J., 1998. Population balance as a tool for understanding particle rate processes. Kona 179–193.

Hounslow, M.J., Ryall, R.L., Marshall, V.R., 1988. A discrete population balance for nucleation, growth and aggregation. A.I.Ch.E. Journal 34 (11), 1821–1832.

Hounslow, M.J., Pearson, J.M.K., Instone, T., 2001. Tracer studies of high-shear granulation: II. Population balance modeling. A.I.Ch.E. Journal 47 (9), 1984–1999.

Immanuel, C.D., Doyle III, F.J., 2003a. Computationally-efficient solution of population balance models incorporating nucleation, growth and coagulation. Chemical Engineering Science 58 (16), 3681–3698.

Immanuel, C.D., Doyle III, F.J., 2003b. Hierarchical multiobjective strategy for particle-size distribution control. A.I.Ch.E. Journal 49 (9), 2383–2399.

Immanuel, C.D., Doyle III, F.J., 2004. Solution technique for multi-dimensional population balance model describing granulation processes. Powder Technology, accepted for publication.

Immanuel, C.D., Cordeiro, C.F., Sundaram, S.S., Doyle III, F.J., 2003. Population balance PSD model for emulsion polymerization with steric stabilizers. A.I.Ch.E. Journal 49 (6), 1392–1404.

Immanuel, C.D., Doyle III, F.J., Stepanek, F., Cameron, I., 2004. Population balance-based modelling of granulation processes. In: Second International Conference on Population Balance Modelling.

Ingram, G.D., Cameron, I.T., 2002. Challenges in multiscale modeling and its application to granulation systems. APCChE 2002/Chemeca 2002, 29 September - 3 October 2002 - Proceedings.

Iveson, S.M., 2002. Limitations of one-dimensional population balance models of wet granulation processes. Powder Technology 124, 219–229.

Iveson, S.M., Litster, J.D., Kapgood, K., Ennis, B.J., 2001. Nucleation, growth and breakage phenomena in agitated wet granulation processes: a review. Powder Technology 117, 3–39.

Kapur, P.C., 1972. Kinetics of granulation by non-random coalescence mechanism. Chemical Engineering Science 27, 1863–1869.

Kapur, P.C., Fuerstenau, D.W., 1969. Coalescence model for granulation. Industrial and Engineering Chemistry Processing Design Development 8, 56–62.

Kaye, B.H., 1997. Powder Mixing. Chapman & Hall, London.

Khan, M.I., 1998. An investigation of powder granulation by experiments and numerical simulation. Ph.D. Thesis, The City University of New York.

Khan, M.I., Tardos, G.I., 1997. Stability of wet agglomerates in granular shear flows. Journal of Fluid Mechanics 347, 347–368.

Kristensen, H.G., Schaefer, T., 1987. Granulation: a review on pharmaceutical wet granulation. Drug Development Industry and Pharmaceuticals 13, 803–872.

Kumar, S., Ramkrishna, D., 1996. On the solution of population balance by discretization—I: a fixed pivot technique. Chemical Engineering Science 51 (8), 1311–1332.

Leuenberger, H., 1994. Moist agglomeration of pharmaceutical processes. In: Chulia, D., Deleuil, M., Pourcelot, Y. (Eds.). Powder Technology and Pharmaceutical Processes, Handbook of Powder Technology, vol. 9. Elsevier, Amsterdam, pp. 337–389.

Lian, G., Thornton, C., Adams, M.J., 1998. Discrete particle simulation of agglomerate impact coalescence. Chemical Engineering Science 53, 3381–3391.

Litster, J.D., 2003. Scaleup of wet granulation processes: science not art. Powder Technology 130, 35–40.

Liu, Y., Cameron, I.T., 2001. A new wavelet-based method for the solution of the population balance equation. Chemical Engineering Science 56, 5283–5294.

Liu, L.X., Litster, J.D., 2002. Population balance modelling of granulation with a physically based coalescence kernel. Chemical Engineering Science 57, 2183–2191.

Liu, L.X., Litster, J.D., Iveson, S.M., Ennis, B.J., 2000. Coalescence of deformable granules in wet granulation processes. A.I.Ch.E. Journal 46 (3), 529–539.

Ljung, L., 1987. System Identification: Theory for the User. Prentice-Hall, Upper Saddle River, NJ.

Ljung, L., 2000. System Identification Toolbox for Use with MATLAB. The Math Works, Natick, MA.

Mahoney, A.W., Doyle III, F.J., Ramkrishna, D., 2002. Inverse problems in population balances: growth and nucleation from dynamic data. A.I.Ch.E. Journal 48 (5), 981–990.

Michaels, J.N., 2003. Toward rational design of powder processes. Powder Technology 138, 1–6.

Miller, S.M., Rawlings, J.B., 1994. Model identification and control strategies for batch cooling crystallisers. A.I.Ch.E. Journal 40 (8), 1312–1327.

Morris, K.R., Nail, S.L., Peck, G.E., Byrn, S.R., Griesser, U.J., Stowell, J.G., Hwang, S.-J., Park, K., 1998. Advances in pharmaceutical materials and processing. Pharmaceutical Science and Technology Today 1, 235–245.

Mort, P.R., Capeci, S.W., Holder, J.W., 2001. Control of agglomerate attributes in a continuous binder-agglomeration process. Powder Technology 117, 173–176.

Nemeth, E.R., Hangos, K.M., Cameron, I.T., 2004a. Hierarchical CPN model-based diagnostics using HAZOP knowledge. Technical Report System and Control Lab SDCL-002/2004, MTA SZTAKI, Budapest, Hungary.

Nemeth, E., Cameron, I.T., Hangos, K.M., 2004b. Diagnostic goal-driven modelling and simulation of multiscale process systems. Computers and Chemical Engineering, in press.

Petzold, L., 1982. A description of DASSL: A differential-algebraic system solver. Proceedings of IMACS World Congress, Montreal, Canada.

Pottmann, M., Ogunnaike, B.A., Adetayo, A.A., Ennis, B.J., 2000. Model-based control of a granulation system. Powder Technology 108, 192–201.

Ramkrishna, D., 2000. Population Balances: Theory and Applications to Particulate Systems in Engineering. Academic Press, San Diego.

Randolph, A.D., Larson, 1988. Theory of Particulate Processes: Analysis and Techniques of Continuous Crystallization. second ed. Academic Press, San Diego.

Salman, A.D., Fu, J., Dorham, D.A., Hounslow, M.J., 2002. Impact breakage of fertilizer granules. Powder Technology 130, 236–359.

Sanders, C.F.W., Willemse, A.W., Salman, A.D., Hounslow, M.J., 2003. Development of a predictive high-shear granulation model. Powder Technology 138, 18–24.

Sastry, K.V.S., 1975. Similarity size distribution of agglomerates during their growth by coalescence in granulation or green pelletization. International Journal of Mineral Processing 2, 187–203.

Schelbach, D., 2000. Development of Granulation Circuit Diagnostics for Gensym's G2 Intelligent Control System. Thesis, Department of Chemical Engineering, Uni of Queensland.

Shahhosseini, S., Cameron, I.T., Newell, R.B., Wang, F.Y., White, E.T., 1997. On-line moisture measurement of sugar using microwave technique. In: Proceedings of the 25th Australia and New Zealand Chemical Engineering Conference, CHEMECA'97, NZ, September.

Smith, M., Matsoukas, T., 1998. Constant number Monte Carlo simulation of population balances. Chemical Engineering Science 53 (9), 1777–1786.

Spielman, L.A., Levenspiel, O., 1965. A Monte Carlo treatment for reaction and coalescing dispersed systems. Chemical Engineering Science 20, 247.

Stepanek, F., 2004. Computer-aided product design: granule dissolution. Chemical Engineering Research Development 82, 1458–1466.

Stepanek, F., Warren, P.B., 2002. Mesoscale modelling of granule pore structure and morphology. In: Proceedings of the 4th World Congress on Particle Technology, Paper No. 247, 21–25 July 2002, Sydney, Australia.

Subero, J., Ning, Z., Ghadiri, M., Thornton, C., 1999. Effect of interface energy on the impact strength of agglomerates. Powder Technology 105 (1–3), 66–73.

Talu, I., Tardos, G.I., Khan, M.I., 2000. Computer simulation of wet granulation. Powder Technology 110, 59–75.

Tardos, G.I., Khan, M.I., Mort, P.R., 1997. Critical parameters and limiting condition in binder granulation of fine powders. Powder Technology 94, 245–258.

Teo, K.L., Goh, C.J., Wong, K.H., 1991. A Unified Computational Approach for Optimal Control Problems. Longman Scientific and Technical, New York.

Thornton, C., Ciomocos, M.T., Adams, M.J., 1999. Numerical simulations of agglomerate impact breakage. Powder Technology 105, 74–82.

van den Dries, K., de Vegt, O., Girard, V., Vromans, H., 2003. Granule breakage phenomena in a high shear mixer: influence of process and formulation variables and consequences on granule homogeneity. Powder Technology 130, 228–236.

Verkoeijen, D., Pouw, G.A., Meesters, G.M.H., Scarlett, B., 2002. Population balances for particulate processes—a volume approach. Chemical Engineering Science 57, 2287–2303.

Vikhansky, A., Kraft, M., 2004. A Monte Carlo method for identification and sensitivity analysis of coagulation processes. Journal of Computational Physics 200, 50–59.

Villermaux, J., 1996. Fifth World Congress of Chemical Engineering. San Diego, USA, pp. 16–23.

Wang, F.Y., Cameron, I.T., 2002. Review and future directions in the modelling and control of continuous drum granulation. Powder Technology 124, 238–253.

Wang, F.Y., Ge, X.Y., Balliu, N., Cameron, I.T., 2004. Optimal control and operation of drum granulation. In: Proceedings of the second International Conference on Population Balance Modelling (PBM 2004), Valencia, Spain, May.

Wang, F.Y., Ge, X.Y., Balliu, N., Cameron, I.T., 2005. Optimal control and operation of drum granulation processes. Chemical Engineering Science, in press.

Watano, S., Numa, T., Koizumi, I., Osako, Y., 2001a. Feedback control in high shear granulation of pharmaceutical powders. European Journal of Pharmaceutics and Biopharmaceutics 52, 337–345.

Watano, S., Numa, T., Miyanami, K., Osako, Y., 2001b. A fuzzy control system of high shear granulation using image processing. Powder Technology 115, 124–130.

Wauters, P.A.L., 2001. Modelling and Mechanisms of Granulation. Ph.D. Thesis, The Delft University of Technology, The Netherlands.

Webb, P.A., Orr, C., 1997. Analytical methods in fine particle technology. Micrometrics Instrument Corporation. http://www.micrometrics.com.

Wildeboer, W.J., 2002. Design and operation of regime separated granulators. Ph.D. Dissertation, University Queensland.

Wright, H., Ramkrishna, D., 1992. Solution of inverse problems in population balances: I. aggregation kinetics. Computers and Chemical Engineering 16 (12), 1019–1038.

Yekeler, M., Ozkan, A., 2002. Determination of the breakage and wetting parameters of calcite and their correlations. Particles and Particle System Characterization 19, 419–425.

Zhang, J., Lister, J.D., Wang, F.Y., Cameron, I.T., 2000. Evaluation of control strategies for fertiliser granulation circuits using dynamic simulation. Powder Technology 108, 122–129.